Molecular Cell
Article

A *Tetrahymena* Piwi Bound to Mature tRNA 3′ Fragments Activates the Exonuclease Xrn2 for RNA Processing in the Nucleus

Mary T. Couvillion,[1] Gergana Bounova,[2] Elizabeth Purdom,[2] Terence P. Speed,[2] and Kathleen Collins[1,*]
[1]Department of Molecular and Cell Biology, University of California at Berkeley, Berkeley, CA 94720-3200, USA
[2]Department of Statistics, University of California at Berkeley, Berkeley, CA 94720-3860, USA
*Correspondence: kcollins@berkeley.edu
http://dx.doi.org/10.1016/j.molcel.2012.09.010

SUMMARY

Emerging evidence suggests that Argonaute (Ago)/Piwi proteins have diverse functions in the nucleus and cytoplasm, but the molecular mechanisms employed in the nucleus remain poorly defined. The *Tetrahymena thermophila* Ago/Piwi protein Twi12 is essential for growth and functions in the nucleus. Twi12-bound small RNAs (sRNAs) are 3′ tRNA fragments that contain modified bases and thus are attenuated for base pairing to targets. We show that Twi12 assembles an unexpected complex with the nuclear exonuclease Xrn2. Twi12 functions to stabilize and localize Xrn2, as well as to stimulate its exonuclease activity. Twi12 function depends on sRNA binding, which is required for its nuclear import. Depletion of Twi12 or Xrn2 induces a cellular ribosomal RNA processing defect known to result from limiting Xrn2 activity in other organisms. Our findings suggest a role for an Ago/Piwi protein and 3′ tRNA fragments in nuclear RNA metabolism.

INTRODUCTION

Ago/Piwi protein complexes are central players in RNA silencing pathways, with bound small RNAs (sRNAs) directing the sequence-specific recognition of target nucleic acids. Cytoplasmic Ago/Piwi RNPs typically induce messenger RNA (mRNA) decay and/or translational repression (Ghildiyal and Zamore, 2009). Nuclear Ago/Piwi RNPs typically guide heterochromatin formation for genome maintenance (Grewal, 2010). Studies in many organisms have revealed that these and other Ago/Piwi cellular functions are carried out by diverse mechanisms. In some cases, Ago/Piwi proteins with slicer activity cleave a target transcript directly (Tolia and Joshua-Tor, 2007). In other cases the mechanisms of Ago/Piwi function depend on partner protein associations. Ago proteins loaded with microRNAs interact with a GW domain protein to promote translational repression and deadenylation (Eulalio et al., 2009). Piwi proteins loaded with animal germline Piwi-interacting RNAs associate with Tudor domain-containing proteins to mediate transposon silencing by RNA degradation and DNA methylation (Juliano et al., 2011). *S. pombe* Ago1 recruits a histone methyltransferase complex to direct heterochromatin formation at centromeres, telomeres, and mating type loci (Bayne et al., 2010; Bühler and Moazed, 2007). *S. pombe* Ago1 and associated factors also have roles in promoting RNAP II termination and DNA release coordinated with the cell cycle (Gullerova and Proudfoot, 2008; Zaratiegui et al., 2011) and in cotranscriptional mRNA degradation at stress-inducible genes (Woolcock et al., 2012). In animals, nuclear Ago/Piwi proteins affect RNAP II transcription at protein-coding genes through mechanisms that are not yet well defined (Burkhart et al., 2011; Cernilogar et al., 2011; Guang et al., 2010; Moshkovich et al., 2011).

Exonucleases are important factors in many RNA silencing pathways. They contribute to sRNA biogenesis (Kawaoka et al., 2011), sRNA turnover (Chatterjee and Grosshans, 2009; Ramachandran and Chen, 2008), Ago/Piwi cleavage product degradation (Orban and Izaurralde, 2005; Souret et al., 2004), and decay of translationally repressed mRNAs (Rehwinkel et al., 2005). The 5′ to 3′ exonuclease activity in these cytoplasmic processes is mediated by members of the XRN nuclease family. However, the nuclear-localized XRN, Xrn2/Rat1, has not been implicated in RNA silencing. Studies in yeast and mammalian cells have demonstrated that Xrn2/Rat1 functions in pre-ribosomal RNA (pre-rRNA) processing and in the degradation of truncated or improperly processed rRNA precursors (Geerlings et al., 2000; Henry et al., 1994; Wang and Pestov, 2011). In addition, Xrn2/Rat1 has roles in RNAP I and RNAP II termination (El Hage et al., 2008; Kaneko et al., 2007; Kawauchi et al., 2008; Kim et al., 2004; Luo et al., 2006; West et al., 2004) and the regulation of productive mRNA synthesis (Brannan et al., 2012; Davidson et al., 2012; Jimeno-González et al., 2010).

The ciliate *Tetrahymena thermophila* encodes a large family of Piwi proteins with distinct expression, localization, and associated sRNAs (Couvillion et al., 2009; Chalker and Yao, 2011). During vegetative culture growth by cell fissions, the *Tetrahymena* germline micronucleus is packaged into heterochromatin while the somatic macronucleus that lacks heterochromatin is expressed. In this stage of the life cycle, several *Tetrahymena* Piwi (Twi) proteins bind 23–24 nt sRNA products of the constitutively expressed and genetically essential Dicer 2, but curiously the only *Tetrahymena* Piwi individually essential for growth is the most divergent family member

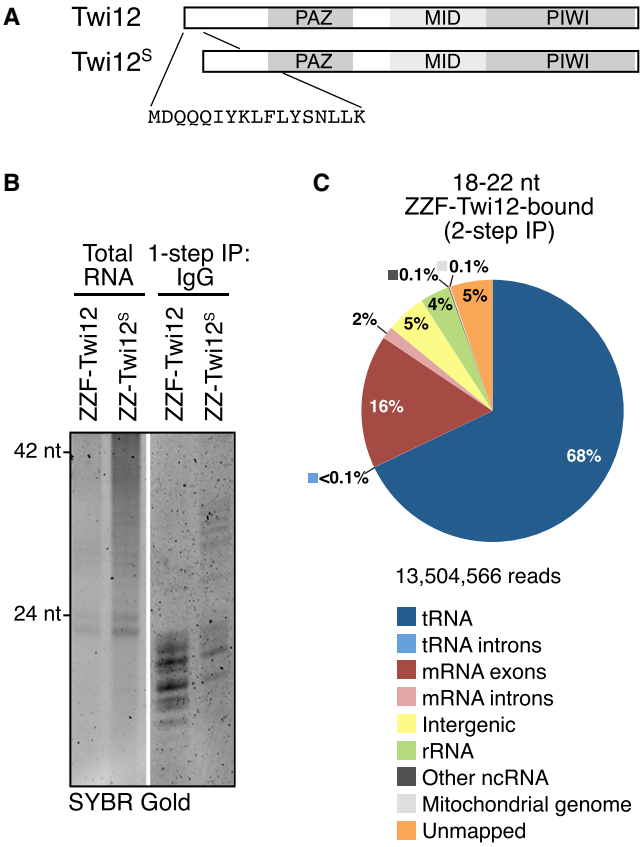

Figure 1. Full-Length Twi12 Binds tRNA Fragments

(A) Schematic of Twi12 compared to Twi12^S, which is truncated by 17 amino acids at the N terminus. See Figure S1 for further description of strains.

(B) RNA copurified with ZZF-Twi12 or ZZ-Twi12^S, resolved by urea-PAGE and stained by SYBR Gold. Total RNA is from the same cells, which express ZZF-Twi12 or ZZ-Twi12^S from the uninduced *MTT1* promoter and do not express endogenous Twi12.

(C) Library composition of sequenced 18–22 nt sRNAs copurified with ZZF-Twi12 expressed from the endogenous *TWI12* promoter, mapped allowing for one internal mismatch and a 3′ overhang of C, CC, or CCA.

See also Figure S1.

Twi12 (Couvillion et al., 2009). Twi12-associated sRNAs are not produced by either *Tetrahymena* Dicer, and Twi12 itself does not conserve slicer catalytic residues (Couvillion et al., 2009; Couvillion et al., 2010). We previously characterized Twi12 association with RNA fragments derived predominantly from the 3′ end of mature transfer RNAs (tRNAs) (Couvillion et al., 2010). These Twi12-bound tRNA fragments are one example of the newly recognized diversity of tRNA processing and tRNA-fragment biology across eukaryotes (Haussecker et al., 2010; Thompson and Parker, 2009). Twi12-bound 18–22 nt tRNA fragment termini are uniform, with the predominant 5′ end in the TΨC loop and the 3′ end at the mature tRNA 3′ terminus. A second, larger size range of Twi12-enriched sRNAs corresponds to tRNA 5′ fragments that are not tightly Twi bound and are thought to be passenger strands from the RNA loading/RNP maturation process (Couvillion et al., 2010).

To elucidate the biological role of Twi12 and its bound tRNA fragments, we have investigated the protein interaction partners of Twi12. We find that Twi12 RNP functions in a multisubunit complex that includes the evolutionarily conserved nuclear 5′ to 3′ exonuclease, Xrn2/Rat1. We demonstrate that *Tetrahymena* Xrn2 functions only in the context of this complex; it is destabilized in vivo and inactive in vitro without sRNA-loaded Twi12. Cellular depletion of *Tetrahymena* Twi12 or Xrn2 inhibits Xrn2-dependent pre-rRNA processing. Our findings uncover a new biological role and mechanism of function for Ago/Piwi RNPs.

RESULTS

Full-Length Twi12 Binds tRNA-Derived Fragments from the 3′ Ends of Mature tRNAs

In a previous study, we reported that overexpressed, tagged Twi12 is bound to tRNA fragments (Couvillion et al., 2010). While creating a *Tetrahymena* strain with Twi12 tagged at its endogenous locus, we discovered an in-frame ATG upstream of the start codon predicted by genome annotation. The corresponding upstream AUG codon is included in the transcript (data not shown). Therefore, we created strains expressing full-length Twi12 for comparison to the original Twi12, now called Twi12 short (Twi12^S) (Figure 1A). We resolved RNAs copurified with each Twi12 by denaturing polyacrylamide gel electrophoresis (PAGE) (Figure 1B). While Twi12^S copurified 18–22 nt and also 25–30 nt RNA populations, Twi12 preferentially copurified the 18–22 nt RNAs, previously shown to be the more tightly bound sRNAs that can be crosslinked to Twi12^S in vivo (Couvillion et al., 2010). We deep sequenced 18–22 nt RNAs copurified with Twi12 N-terminally tagged with two Protein A domains (ZZ), a Tobacco etch virus (TEV) protease cleavage site, and three FLAG peptide (F) sequences (ZZF-Twi12) expressed at the endogenous *TWI12* promoter. We found that the majority of reads mapped to tRNAs without any evident biases across different tRNA molecules (Figure 1C and data not shown). Thus, like Twi12^S, Twi12 selectively copurifies specific bound fragments of tRNAs.

Twi12 is essential for growth; therefore the *TWI12* locus cannot be replaced by a drug-resistance cassette in a wild-type background (Couvillion et al., 2009). However, in the presence of a transgene expressing ZZF-Twi12, the endogenous *TWI12* locus could be fully replaced (Figure S1A available online), indicating that tagged Twi12 is functional. ZZ-tagged Twi12^S (ZZ-Twi12^S) transgene expression can also substitute for endogenous Twi12 (Couvillion et al., 2010), but unlike expression of tagged full-length Twi12, cellular expression of only tagged Twi12^S slowed culture growth in rich medium (Figure S1B). Accordingly, we detected endogenous untagged Twi12 migrating with Twi12 rather than Twi12^S (Figure S1C).

Because Twi12^S could have reduced function, additional characterization of associated sRNAs was done for tagged full-length Twi12. Eukaryotic tRNAs are posttranscriptionally modified by 3′-terminal untemplated CCA addition. Therefore, in mapping reads we allowed for 3′-terminal mismatches of C, CC, or CCA. About 75% of tRNA-derived sRNA reads contain these untemplated nucleotides, compared to less than 10% of

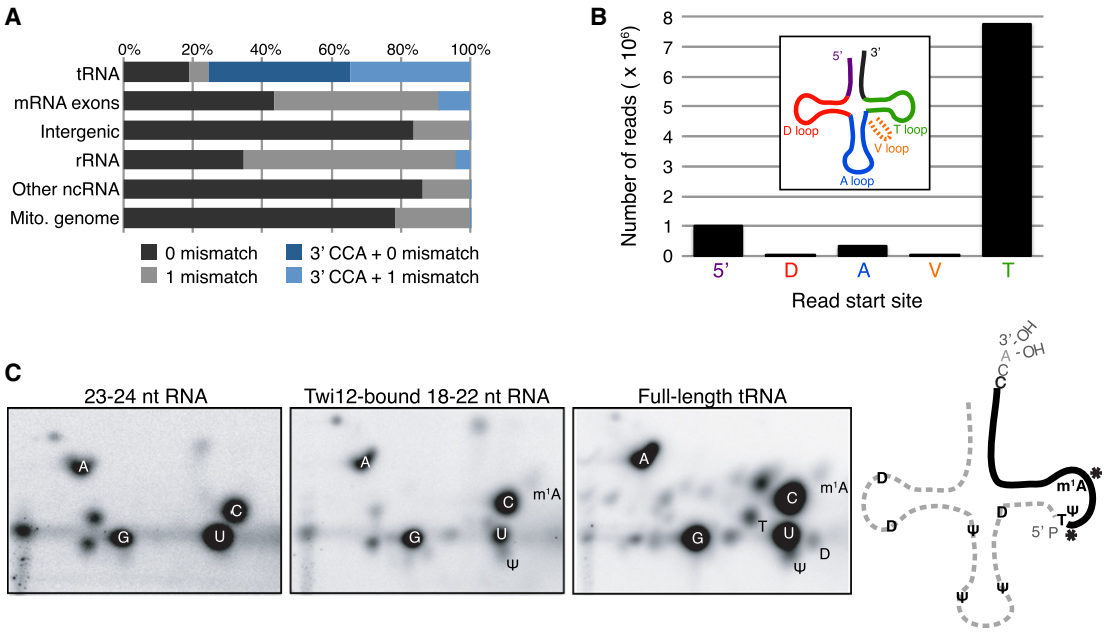

Figure 2. Twi12-Bound sRNAs Are Derived from the 3′ Ends of Mature tRNAs

(A) Annotated reads in each category analyzed for the fraction that map perfectly (black), with one mismatch (gray), or with a 3′ overhang of C, CC, or CCA (blue and light blue, see key). Reads annotated as mRNA and rRNA are most likely misannotated.

(B) Plot showing number of reads with 5′ ends at each tRNA location: 5′ end, D stem loop, anticodon stem loop (A), variable stem loop (V), or TΨC stem loop (T).

(C) Two-dimensional thin layer chromatographic analysis of ^{32}P 5′ monophosphate-labeled nucleosides. The diagram at right shows the positions of the conserved tRNA base modifications that are indicated in the chromatographs. The solid black line indicates the Twi12-bound fragment. Asterisks indicate modified base positions in the Twi12-bound fragment that are pseudouridine (Ψ) or 1-methyl adenosine (m^{1}A).

the reads in all other categories (Figure 2A), which result from a mixture of reads mapping to unannotated tRNAs and misannotated reads. Reads were first mapped allowing for no internal mismatch, and then unmapped reads were mapped allowing for one mismatch. For reads mapping to annotated tRNA, mismatches were only allowed at positions that we annotated as putative base modification sites (see the Supplemental Experimental Procedures). Analysis of the position of reads across tRNA lengths confirmed that the majority are 3′ fragments starting at the pseudouridine (Ψ) in the TΨC loop and ending at the mature tRNA 3′ end (Figures 2B and 2C and data not shown).

Mature tRNA base modifications are important for folding and/or activity in translation (Phizicky and Alfonzo, 2010). To determine whether Twi12-bound tRNA fragments contain modified bases, we used two-dimensional thin-layer chromatography to compare labeled nucleosides from the Twi12-bound sRNAs to those of full-length mature tRNAs and the bulk 23–24 nt sRNAs, which are mostly bound to Twi2 (Figure 2C). Consistent with their processing from functional mature tRNAs, Twi12-bound 18–22 nt RNAs contained Ψ and 1-methyladenosine (m^{1}A), the two conserved modifications found in the T loop of tRNAs (Figure 2C, middle panel and schematic at right). These sRNAs did not contain thymidine (T) or dihydrouridine (D), which are clearly identifiable in labeled nucleosides from full-length tRNA (Figure 2C, right panel). The conserved m^{1}A modification at tRNA position 58 (Twi12-bound sRNA position 4) is also evident in sequence reads, because this base is often misread by reverse transcriptase during library preparation, resulting in a relatively high frequency of mismatch at this position (see the Supplemental Experimental Procedures). Together, presence of the 3′ untemplated CCA and the base modifications provide strong support for the conclusion that Twi12-bound sRNAs derive from mature tRNAs.

Twi12 Forms a Nuclear Complex with Xrn2 and Tan1

To gain insight into the function of Twi12, we next investigated interacting proteins. SDS-PAGE and silver staining after a two-step immunoprecipitation (IP) of ZZF-Twi12 expressed from the endogenous *TWI12* promoter revealed several coenriched polypeptides with apparent masses between 85 and 120 kDa (Figure 3A). Mass spectrometry identified two proteins in addition to Twi12, each with significant peptide coverage and each not found in the mock-purification control: a 12.3 kDa protein with no homologs that we named Tan1 (*T*wi-*a*ssociated *n*ovel 1) and a 126 kDa protein containing a 5′ to 3′ monophosphate-dependent exonuclease domain (Figure 3B). The *Tetrahymena* genome encodes three putative proteins with a 5′ to 3′ exoribonuclease domain. Two are most similar to Xrn1 from yeast and human, and, consistent with Xrn1-like function, they have cytoplasmic localization (Douglas Chalker, personal communication), whereas the one identified in association with Twi12 is more similar to human XRN2 and yeast Rat1, and thus we named it Xrn2.

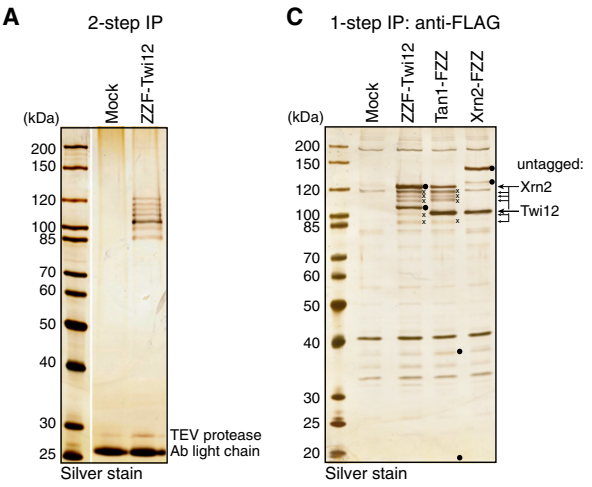

B

TTHERM ID	Protein	Unique peptides	Percent coverage	MW (kDa)	pI	Domains
00145270	Xrn2	29	23	126	6.3	XRN 5′ to 3′ exo
00653810	Twi12	29	37	101	7.7	PAZ, PIWI
00399370	Tan1	7	25	12	9.0	DUF3469

Figure 3. Twi12 Interacts with Xrn2 and Tan1

(A) SDS-PAGE and silver staining after two-step IP of ZZF-Twi12 expressed from the endogenous locus. The first step was IgG IP and TEV protease elution, and the second step was anti-FLAG IP and urea elution.

(B) Table of ZZF-Twi12-associated proteins identified by mass spectrometry. See also Figures S2A and S2B.

(C) SDS-PAGE and silver staining after one-step IP of the proteins identified by mass spectrometry. Filled circles indicate the tagged protein in each lane, which runs as two bands (ZZF-tagged and F-tagged) because of proteolytic clipping between the tag segments. Labels at right indicate the migration positions of untagged proteins, and small Xs mark Xrn2 proteolysis fragments. Note that tagged Tan1 does not silver stain strongly. See also Figures S2C and S2D.

(D) Illustrated model of TXT with bound sRNA. Asterisks on the line representing sRNA indicate base modifications. Direct interaction of Tan1 with Twi12 is not established.

See also Figure S2.

To verify the interaction of Twi12 with Tan1 and Xrn2, we created cell lines expressing Tan1 or Xrn2 tagged at their endogenous loci. IP of Tan1-FZZ and Xrn2-FZZ confirmed their interaction with Twi12 and each other (Figure 3C). We refer to the *T*wi12/*X*rn2/*T*an1 complex as TXT (Figure 3D; see below for analysis of sRNA in TXT). No other proteins associated with any of the three subunits were detectable by silver staining. The ladder of silver-stained bands between 85 and 120 kDa visible with IP of Twi12 was also evident with IP of Tan1 but not C-terminally tagged Xrn2 (Figure 3C). We therefore suspect that the ladder derives from proteolysis of Xrn2 near its C terminus.

To test whether Tan1 and Xrn2, like Twi12, are essential for *Tetrahymena* growth, we attempted to replace their endogenous loci with a drug-resistance cassette (*neo2)* on all chromosomes in the somatic macronucleus by phenotypic assortment. *TAN1* could be fully replaced by *neo2* (Figure S2A), and therefore it is not essential. *XRN2* could be only partially replaced (Figure S2B), suggesting that it is essential. We used Tan1 knockout (KO) cell lines to investigate the function of Tan1 in TXT. IP of Xrn2 in the Tan1 KO background still recovered Twi12, indicating that Tan1 is not required for Twi12/Xrn2 association (Figure S2C). Additionally, IP of Twi12 in the Tan1 KO background still recovered 18–22 nt RNA, indicating that Tan1 is not required for sRNA binding (Figure S2D).

Xrn2/Rat1 homologs are generally nuclear, so the interaction of Twi12 with Xrn2 was surprising because overexpressed ZZ-Twi12^{S} is predominantly cytoplasmic (Couvillion et al., 2009). However, indirect immunofluoresence (IF) to detect ZZF-Twi12, Tan1-FZZ, and Xrn2-FZZ expressed from their endogenous promoters revealed each of them to be predominantly nuclear. Each protein was enriched in the expressed macronucleus (Figure 4A), consistent with the assembly of these three subunits as a TXT complex. IF analysis of ZZF-Twi12 expressed from the cadmium-inducible *MTT1* promoter revealed mostly nuclear localization when only slightly overexpressed (without promoter induction) but predominantly cytoplasmic localization when highly overexpressed (data not shown), accounting for the previously reported localization of ZZ-Twi12^{S}.

Xrn2 Has 5′ Monophosphate-Dependent Exonuclease Activity

Using purified TXT, we assayed for the expected 5′ monophosphate-dependent single-stranded RNA exonuclease activity of XRN family enzymes (Jinek et al., 2011). TXT purified by ZZF-Twi12, Tan1-FZZ, or Xrn2-FZZ did degrade 5′ monophosphorylated RNA, e.g., 5.8S rRNA, but not 5′ triphosphorylated RNA, e.g., 5S rRNA, from a mixture of purified, low-molecular-weight *Tetrahymena* cellular RNA (Figure 4B). We conclude that Xrn2 has 5′ monophosphate-dependent activity in vitro in the context of TXT.

The Xrn2 homolog in yeast, Rat1, is stabilized for catalytic activity in vitro by the small associated protein Rai1 (Xue et al., 2000), which has a pyrophosphohydrolase activity that converts triphosphorylated RNAs to monophosphorylated Rat1 substrates (Xiang et al., 2009). Although we could not identify any sequence or structural similarity between Tan1 and Rai1, we tested for Tan1 pyrophosphohydrolase activity. None could be detected, either for recombinant Tan1 purified from *E. coli* or for Tan1 in the context of TXT (Figure S3A). Furthermore, Tan1 was not required for Xrn2 exonuclease activity in vitro (Figure S3B).

One potential function of Xrn2 in TXT is to trim anticodon loop-cleaved tRNAs to produce the 5′ ends of the Twi12-bound tRNA fragments. To test this hypothesis, we used N-terminally tagged Xrn2 (ZZF-Xrn2), which cannot functionally substitute for untagged Xrn2 in vivo (data not shown) and which has reduced catalytic activity in vitro (Figure 4B). TXT complexes containing

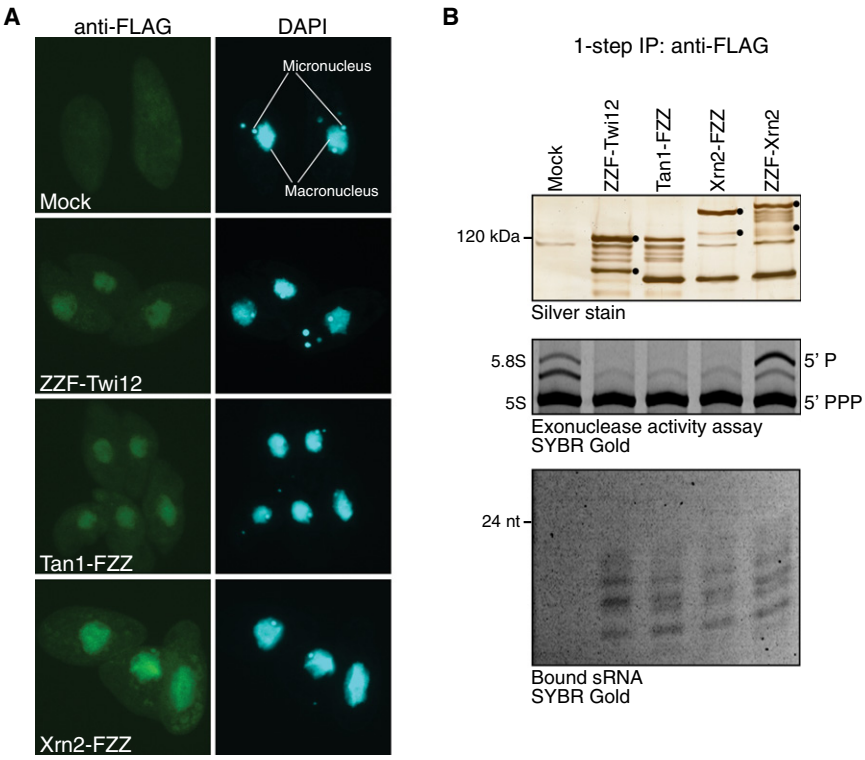

Figure 4. TXT Is a Nuclear Complex with 5′ Monophosphate-Dependent Exonuclease Activity

(A) Indirect IF for each subunit in TXT.

(B) Nuclease activity assay on TXT purified by each subunit. Top: silver stained proteins after one-step IP. Middle: RNA after in vitro incubation with TXT. Note that N-terminally tagged Xrn2 is catalytically inactive. Bottom: sRNAs associated with each population of TXT in vivo.

See also Figure S3 for analysis of a potential Tan1 activity.

ZZF-Xrn2 purified the identical size range and amount of 18–22 nt sRNAs as the TXT complexes purified by ZZF-Twi12, Tan1-FZZ, or Xrn2-FZZ, each of which contained active Xrn2 (Figure 4B, bottom panel), suggesting that Xrn2 catalytic activity is not required for Twi12-bound sRNA maturation within its TXT complex. Furthermore, the similar amounts of 18–22 nt sRNAs enriched by TXT purification using each separately tagged subunit indicate that sRNA is an integral component of the TXT RNP.

RNA Binding Is Required for Twi12 Nuclear Import

Twi12 is a divergent Ago/Piwi protein family member (Couvillion et al., 2009; Seto et al., 2007), leaving open the possibility that sRNA binding is a vestigial characteristic not essential to Twi12 function. To address the significance of Twi12 sRNA binding, we made cell lines expressing tagged Twi12 sequence variants. In Twi12^{Y524E}, a single amino acid substitution replaces a conserved tyrosine (Y) with a negatively charged glutamate (E) (Figure S4A) in the binding pocket for the sRNA 5′ phosphate (Ma et al., 2005). Similar phosphate mimicry was shown to abrogate sRNA binding by human AGO2 (Rüdel et al., 2011). Another conserved residue in the 5′ phosphate binding pocket is a glutamine (Q) that Twi12 lacks; Twi12 instead has a serine (S) at the analogous position (Figure S4A). The structure of the *Archaeoglobus fulgidas* Piwi with bound sRNA (Ma et al., 2005; Figure S4B) shows this Q, Q137, at a position where it could sterically hinder loading of a 5′-extended precursor (Figure S4B) required as a biogenesis step in our model for Twi12 loading with full-length or anticodon-nicked tRNA (Couvillion et al., 2010). Therefore, we also made cell lines expressing tagged Twi12^{S540Q}, which has a single amino acid substitution restoring the conserved Q.

Two different cell lines were made to express each Twi12 sequence variant described above: one for overexpression, in which the tagged Twi12 is expressed from the *MTT1* cadmium-inducible promoter at the ectopic *BTU1* locus, and one in which the tagged Twi12 is expressed from the endogenous promoter at the endogenous locus. Consistent with disruption of critical recognition of the sRNA 5′ monophosphate, ZZF-Twi12^{Y524E} did not associate with sRNA whether slightly overexpressed from the uninduced *MTT1* promoter (Figure 5A) or expressed at or below endogenous level from the endogenous *TWI12* promoter (Figure S4C). We note that unloaded Twi12 may be more susceptible to proteolysis than Twi12 RNP in vivo and/or in cell lysate, as observed for *Drosophila* Piwi (Olivieri et al., 2010), because less ZZF-Twi12^{Y524E} was purified than ZZF-Twi12 or ZZF-Twi12^{S540Q} from an equivalent amount of cell extract (Figures 5A and S4C). Unlike ZZF-Twi12^{Y524E}, ZZF-Twi12^{S540Q} retained sRNA binding (Figures 5A and S4C). Immunofluorescence analysis revealed that wild-type ZZF-Twi12 and ZZF-Twi12^{S540Q} accumulated in the macronucleus, while ZZF-Twi12^{Y524E} and ZZF-Twi12^{S} (with an altered sRNA size profile; Figure 5A, and see also ZZ-Twi12^{S} sRNAs in Figure 1B) accumulated to higher levels in the cytoplasm, whether slightly overexpressed from the uninduced *MTT1* promoter (Figure 5B) or expressed at or below endogenous level from the endogenous *TWI12* promoter (Figure S4D). Consistent with a loss of function, ZZF-Twi12^{Y524E} expression did not allow for KO of endogenous *TWI12*; in contrast, ZZF-Twi12^{S540Q} expression did (data not shown). We conclude that sRNA binding is a prerequisite for Twi12 nuclear localization and physiological function.

Depletion of Twi12 or Xrn2 Induces a Pre-rRNA Processing Defect

To test whether *Tetrahymena* Xrn2 and Twi12 cellular functions are interrelated, as suggested by their stable physical association, we made inducible knockdown (iKD) cell lines for conditional expression of each protein. First, F-tagged transgenes encoding each protein were separately integrated at the *MTT3*

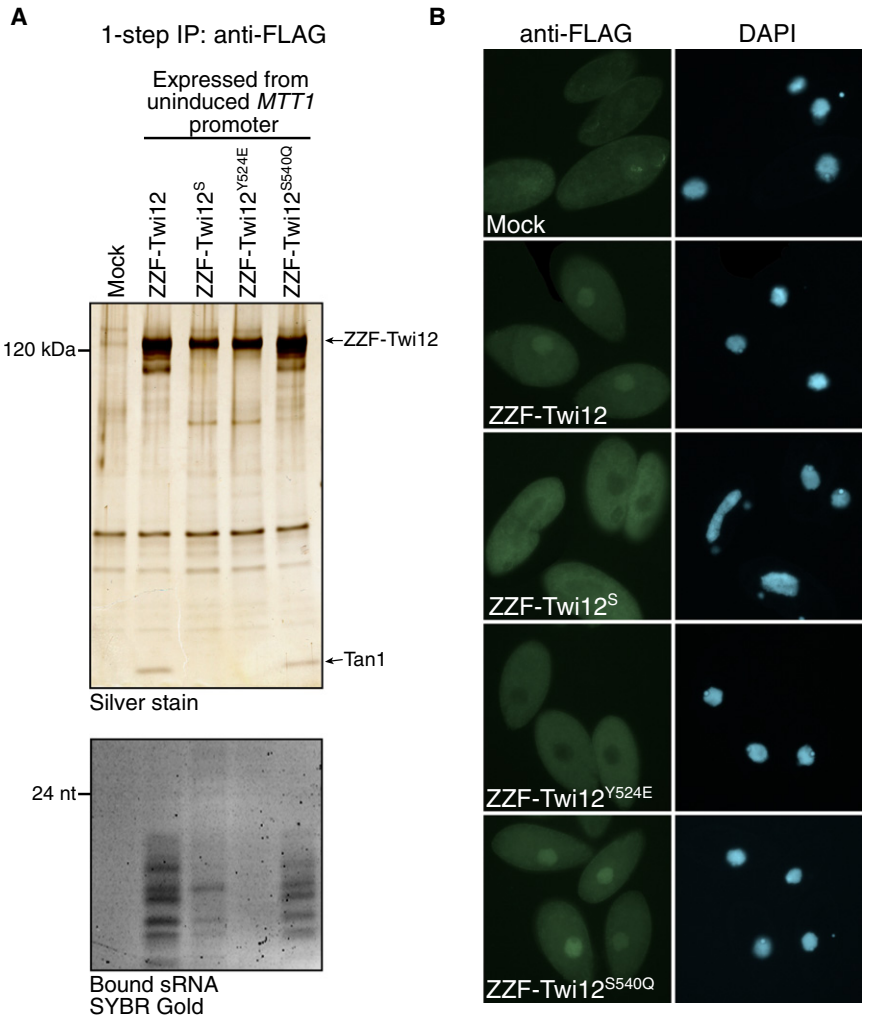

Figure 5. Twi12 Nuclear Localization Is Dependent on sRNA Binding

(A) SDS-PAGE and silver staining after one-step IP of ZZF-Twi12 wild-type and variants expressed from the uninduced *MTT1* promoter (top), with SYBR Gold staining of associated sRNA (bottom). (B) Indirect IF for ZZF-Twi12 wild-type and variants expressed from the uninduced *MTT1* promoter. See also Figure S4.

locus under the control of the cadmium-inducible *MTT3* promoter (Figures 6A and S5). This locus was chosen because of its low basal (uninduced) expression (Miao et al., 2009). Subsequently, replacement of the endogenous *TWI12* or *XRN2* locus with a drug-resistance cassette could be driven to complete assortment when cultures were grown in the presence of cadmium to induce transgene expression, as assessed by Southern blot hybridization (Figure S5). Cells were maintained in a cadmium concentration that supported near endogenous levels of protein expression, as judged by western blotting of ZZF-Twi12 expressed from the endogenous promoter (data not shown). Within six to seven population doublings after removal of cadmium, culture growth dramatically slowed and protein accumulation level diminished to less than 20% for F-Twi12 or less than 50% for Xrn2-F of the protein level in cells grown in cadmium, relative to a tubulin loading control (Figure 6A).

A well-established role for Xrn2/Rat1 in yeast and human cells is in the 5′-3′ trimming required to remove internal transcribed spacer regions of the primary rRNA transcript after its initial endonucleolytic cleavage (Geerlings et al., 2000; Henry et al., 1994; Wang and Pestov, 2011). To investigate the impact of Twi12 or Xrn2 depletion on *Tetrahymena* pre-rRNA processing, we probed total RNA from wild-type, Twi12 iKD, and Xrn2 iKD cells using an oligonucleotide complementary to the internal transcribed spacer 5′ of mature 5.8S rRNA (Figure 6B, top), which is a substrate for Xrn2 processing in other organisms (Henry et al., 1994). Strikingly, pre-rRNA processing intermediates increased in accumulation in Twi12 iKD and Xrn2 iKD cells upon depletion of either protein (Figure 6B). In parallel, mature 5.8S rRNA accumulation was reduced, a change that was particularly evident for the more effective TXT depletion by shut off of Twi12 (Figures 6A and 6B). In contrast, there was no change in the accumulation of mature 17S rRNA (Figure 6B), which is not known to be processed by Xrn2. No pre-rRNA processing phenotypes were observed in wild-type cells across a range of growth rate (data not shown), indicating that the phenotype is specific to depletion of TXT.

Total RNA from wild-type, Twi12 iKD, and Xrn2 iKD cells was also probed to detect *RPL21* mRNA, an abundant ribosomal protein mRNA typically used as a *Tetrahymena* RNA loading control. We were surprised to detect increased accumulation of this mRNA in Twi12 iKD and Xrn2 iKD cells depleted for TXT (Figure 6B). Unlike *RPL21* mRNA, the mitochondrially encoded *YMF66* mRNA was unchanged in accumulation upon Twi12 or Xrn2 depletion (Figure 6B). There was also no impact of Twi12 or Xrn2 depletion on the accumulation of tRNAs processed from primary transcripts of RNAP III (Figure 6B). However, a full-length or near full-length rRNA precursor transcript of RNAP I was increased upon Twi12 or Xrn2 depletion (Figure 6B, asterisk). The combination of these results raises the possibility that *Tetrahymena* TXT has role(s) similar to human and yeast Xrn2/Rat1 in the cotranscriptional regulation of RNAP I and RNAP II (Brannan et al., 2012; Davidson et al., 2012; El Hage et al., 2008; Jimeno-González et al., 2010; Kaneko et al., 2007; Kawauchi et al., 2008; Kim et al., 2004; Luo et al., 2006; West et al., 2004). However, future experiments will be necessary to investigate any cotranscriptional regulatory function of TXT.

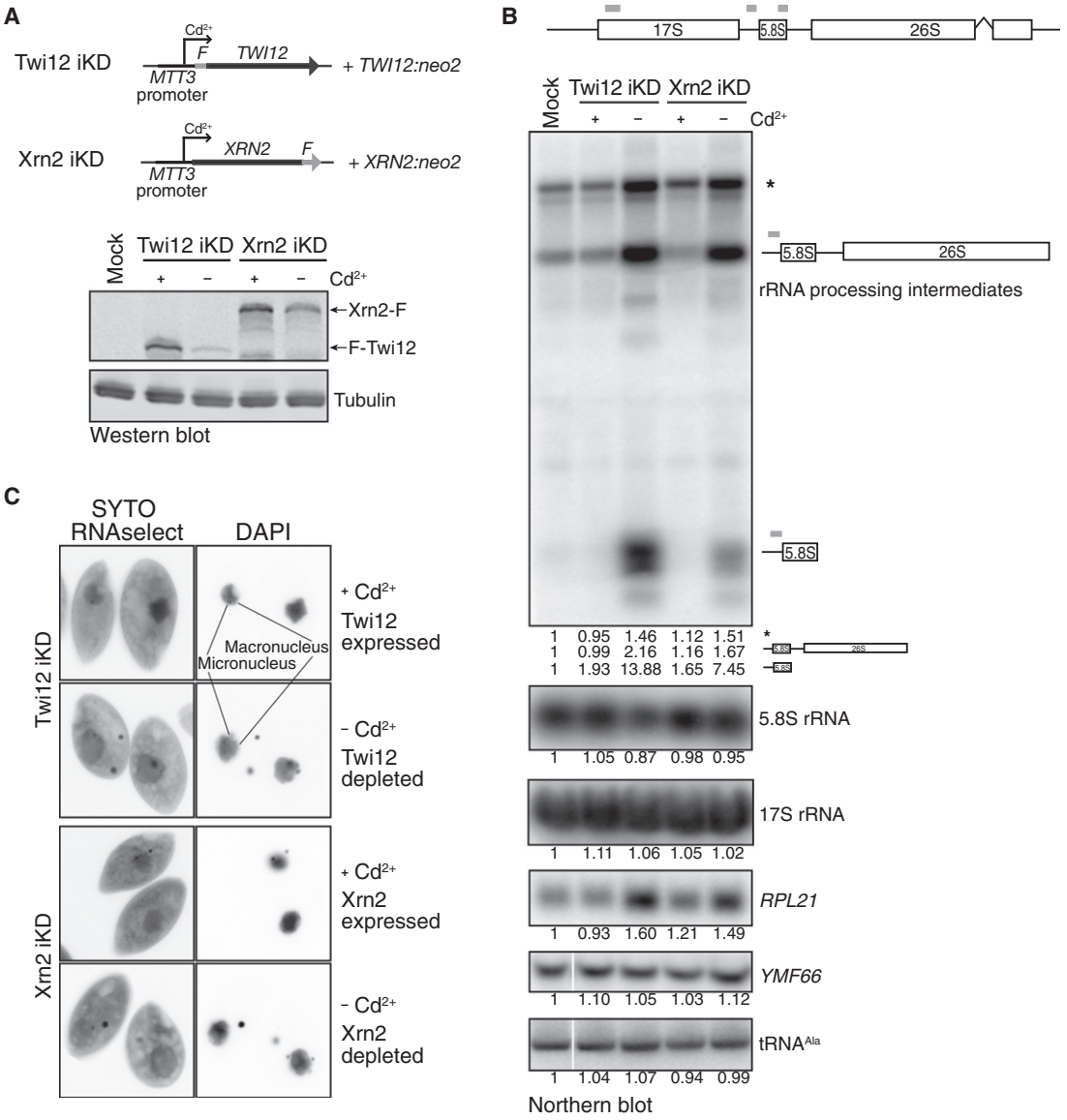

Figure 6. Depletion of Twi12 or Xrn2 Induces a Pre-rRNA Processing Defect

(A) Twi12 or Xrn2 depletion was achieved by cadmium removal from cells with the genotypes schematized at top (see also Figure S5). Bottom: Western blot probed with anti-FLAG and anti-tubulin, with loading normalized for cell equivalents of whole-cell extract.

(B) Top: schematic of the *Tetrahymena* rRNA RNAP I transcript. Gray lines show positions of probes, and the 26S rRNA intron is also shown. Bottom: Northern blot analysis of total RNA samples normalized by cell equivalents. Blots were made from two gels loaded with the same RNA samples; both blots were probed for *RPL21* mRNA as a control for equivalent loading. The asterisk indicates full-length or near full-length pre-rRNA transcript. Numbers below each panel indicate signal intensity normalized to that of wild-type cells.

(C) SYTO RNASelect staining of Twi12 iKD and Xrn2 iKD cells cultured with and without cadmium. Note that both RNA and DNA are stained by SYTO RNASelect in these paraformaldehyde-fixed cells.

See also Figure S5.

To investigate TXT-dependent cellular RNA accumulation using another approach, we stained whole cells with the fluorescent dye SYTO RNASelect. Using cells fixed with paraformaldehyde before staining, we found that the dye stains DNA as well as RNA, as evidenced by staining of transcriptionally silent micronuclei (Figure 6C). Twi12- or Xrn2-depleted cells had notably increased staining at the macronuclear periphery, which is evident as an enlargement of the stained macronuclear volume compared to that stained by DAPI (Figure 6C). This increased staining mirrors the localization of *Tetrahymena* nucleoli (Gorovsky, 1973), which are positioned just beneath the macronuclear envelope around the DAPI-staining central area of bulk chromatin. We suggest that the change in pattern of SYTO RNASelect staining upon depletion of Twi12 or Xrn2 (Figure 6C)

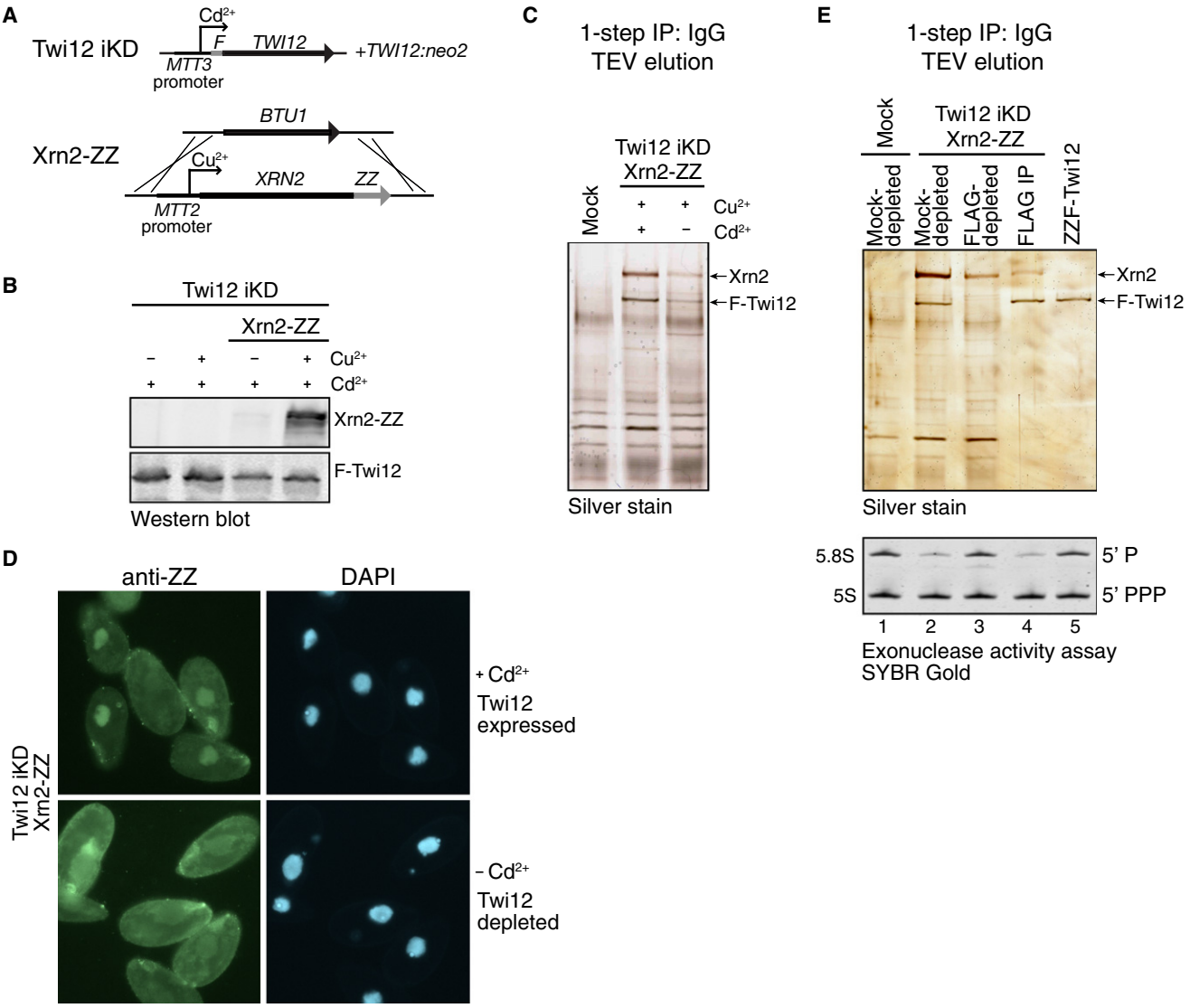

Figure 7. Xrn2 Requires Twi12 for Accumulation, Nuclear Localization, and Activity

(A) Genetic strategy for generation of the cell line in which Xrn2 is tagged in the Twi12 iKD background.

(B) Western blot probed with IgG or anti-FLAG, with loading normalized for cell equivalents of whole-cell extract.

(C) SDS-PAGE and silver staining after one-step IgG IP of Xrn2-ZZ from cell extracts.

(D) Indirect IF for Xrn2-ZZ in cells with Twi12 expressed (+Cd^{2+}) or depleted (−Cd^{2+}). Note that there is some cell-to-cell variability in transgene expression level.

(E) Nuclease activity. Top: silver stained samples after purification and depletion as indicated. Bottom: RNA after in vitro incubation with each purified sample.

reflects the greatly increased abundance of rRNA processing intermediates detected at the molecular level (Figure 6B).

Twi12 Is Necessary for Xrn2 Accumulation, Localization, and Activity

We next investigated how Twi12 influences Xrn2 activity at a biochemical level. To detect and purify Xrn2 before and after conditional depletion of Twi12, we introduced a transgene encoding ZZ-tagged Xrn2 (Xrn2-ZZ) in the Twi12 iKD line (Figure 7A). Xrn2-ZZ was expressed under the control of the copper-inducible *MTT2* promoter (Díaz et al., 2007). Xrn2-ZZ level was greatly increased upon addition of copper to the growth medium (Figure 7B). This allowed us to independently vary the cellular expression of Xrn2 and Twi12 by adding copper and/or removing cadmium from the growth medium.

Even if Xrn2-ZZ was overexpressed by copper addition simultaneously with Twi12 depletion by cadmium removal, we were unable to IP an excess of Xrn2-ZZ over F-Twi12 from whole-cell extract (Figure 7C). These results suggest that Xrn2 cellular stability depends on its association with Twi12. Consistent with this conclusion, Twi12 depletion reduced the amount of functional, nuclear Xrn2-ZZ monitored by IF (Figure 7D) and also total

Xrn2-ZZ monitored by western blot (data not shown). Based on the stabilizing influence of the proteasome inhibitor MG132 (see below), we suggest that Xrn2 that is not associated with Twi12 is degraded by protein turnover in the cytoplasm. We propose that Twi12, once loaded with a tRNA fragment, binds Xrn2 to facilitate Xrn2 cellular accumulation and nuclear import through formation of TXT.

Finally, we tested whether Twi12 is required for Xrn2 catalytic activity. To obtain Xrn2 without other TXT subunits, we exploited cells overexpressing Xrn2-ZZ in the Twi12 iKD background (Figures 7A and 7B) with Xrn2-ZZ expression induced in the presence of the proteasome inhibitor MG132. ZZ-Xrn2 IP was performed by binding to IgG agarose, with extract from cells overexpressing Xrn2-ZZ or cells lacking tagged protein (mock). Subsequently, IgG-purified Xrn2 was depleted of F-Twi12 with FLAG antibody resin (Figure 7E, lane 3). In parallel, as a control, IgG-purified mock and Xrn2 samples were mock depleted at the FLAG antibody resin step to control for incubation time as well as nonspecifically enriched activities and/or inhibitors (Figure 7E, lanes 1 and 2). All of these depleted samples, the eluate from the FLAG antibody resin containing enriched TXT complex (Figure 7E, lane 4) and F-Twi12 from ZZF-Twi12-overexpressing cells (Figure 7E, lane 5) were tested for exonuclease activity. Strikingly, Xrn2 lacking associated Twi12 had no detectable exonuclease activity (Figure 7E, lane 3). TXT, on the other hand, selectively degraded RNA with a 5′ monophosphate (Figure 7E, lane 4), and, as expected, F-Twi12 without Xrn2 had no nuclease activity (Figure 7E, lane 5). These findings strongly suggest that *Tetrahymena* Xrn2 functions only in association with Twi12 RNP.

DISCUSSION

TXT Assembly and Nuclear Import

Analogous to the RNA loading of many Ago/Piwi proteins, we suggest that Twi12 initially binds a double-stranded RNA structure formed by the mature tRNA acceptor and TΨC stems (Couvillion et al., 2010). RNP maturation would then involve tRNA nicking and passenger-strand degradation and/or unwinding activities. The nuclease(s) responsible for trimming Twi12-bound tRNAs could be broad rather than tRNA-specific in their substrate cleavage specificity, as shown for the *Tetrahymena* RNase T2 enzymes involved in starvation-induced tRNA cleavages (Andersen and Collins, 2012). An N-terminally truncated form of Twi12 ($Twi12^S$) shows increased retention of tRNA 5′ fragments under native purification conditions (Couvillion et al., 2010; Figure 1B). These 5′ fragments probably represent bona fide loading intermediates, because the Argonaute N-terminal domain has been established to be important for unwinding the sRNA duplex during loading (Kwak and Tomari, 2012). Twi12-bound sRNAs are scarce compared to mature tRNAs, so it seems likely that only a small fraction of the mature tRNA pool is degraded by a mechanism involving Twi12. The evolutionary specialization of Twi12 loading with tRNAs could in part reflect the expedience of tRNA as an available base-paired cytoplasmic RNA, rather than a biologically selected role for Twi12 in tRNA regulation. Or, if tRNA availability for Twi12 loading changes with cellular conditions, Twi12 specialization for tRNA binding could be part of a physiological regulation of ribosome biogenesis.

Two lines of evidence support the hypothesis that Twi12 nuclear import depends on sRNA binding and maturation. First, Twi12 defective for sRNA binding is not imported (Figures 5B and S4C). Second, $Twi12^S$, which is impaired in duplex unwinding, remains predominantly cytoplasmic (Figures 5B and S4C). Nuclear import dependent on RNA binding has been reported for the Ago/Piwi proteins *Tetrahymena* Twi1, *C. elegans* NRDE-3, mouse Miwi2, *Drosophila* Piwi, and *Arabidopsis* AGO4 (Ishizu et al., 2011; Ye et al., 2012). Also, for Twi1 and AGO4, unwinding of the bound sRNA duplex is an established prerequisite for nuclear import (Noto et al., 2010; Ye et al., 2012). It seems likely to be a general principle that sRNA loading and RNP maturation provide a checkpoint for import of nuclear-localized Ago/Piwi proteins.

The TXT complex with Twi12 and Xrn2 also contains Tan1 (Figure 3). Tan1 is not necessary for Twi12 nuclear accumulation (data not shown), suggesting that Tan1 functions downstream of sRNA loading. Although Tan1 is part of the functional TXT RNP (Figure 4B), unlike Twi12 and Xrn2 it is not a genetically essential subunit (Figure S2A). Furthermore, Tan1 KO does not impose an obvious slow-growth phenotype (data not shown). Tan1 was not critical for Xrn2 catalytic activity in vitro (Figure S3), but it is possible that Tan1 stimulates Xrn2 degradation of a subset of TXT substrates whose altered accumulation does not confer a cellular disadvantage under typical laboratory growth conditions.

TXT Function

Our results suggest that Twi12 functions as an essential activator of Xrn2. All of the depletion phenotypes of Twi12 and Xrn2 are consistent with known roles for Xrn2 in pre-rRNA processing or cotranscriptional RNA degradation. Although the role of an Ago/Piwi protein in Xrn2 activation was unanticipated, it could be general. Indeed, Ago/Piwi proteins have been implicated in pre-rRNA processing in human cells (Liang and Crooke, 2011) and in transcriptional or cotranscriptional silencing of protein-coding genes in *C. elegans*, *S. pombe*, and *Drosophila* (Cernilogar et al., 2011; Guang et al., 2010; Moshkovich et al., 2011; Woolcock et al., 2012). These mechanisms of silencing could depend on direct RNAP II interaction and/or cotranscriptional RNA degradation.

Xrn2 homologs have diverse functions. For this reason, we initially expected *Tetrahymena* Xrn2 to interact with protein partners in addition to Twi12 and Tan1 and for its role in TXT to involve the biogenesis of precisely processed Twi12-bound tRNA fragments. On the contrary, IP of Xrn2 did not copurify any detectable proteins other than Twi12 and Tan1 (Figures 3C and S2C). Furthermore, Xrn2 catalytic activity was not required for the associated Twi12 RNA loading (Figure 4B), although subunit exchange among assembled TXT complexes would complicate the interpretation of this result. Combining this with our inability to IP Xrn2 free of Twi12 without proteasome inhibition and with the Twi12 requirement for Xrn2 catalytic activity (Figures 7C and 7E), we suggest that *Tetrahymena* Xrn2 may not have functions beyond those mediated by TXT.

Twi12-Dependent Accumulation, Localization, and Activity of Xrn2

In budding and fission yeasts, the Xrn2 ortholog Rat1 gains conformational stability and improved activity through direct interaction with its cofactor Rai1 (Xiang et al., 2009; Xue et al., 2000). The amino acid side chains that contribute to the Rai1-Rat1 interface are conserved across fungal species but not all eukaryotes, consistent with a lack of human Xrn2 protein-protein interaction with the proposed human Rai1 ortholog Dom3Z (Xiang et al., 2009). Structural alignment of *Tetrahymena* Xrn2 with *S. pombe* Rat1 suggests that *Tetrahymena* Xrn2 also does not conserve the yeast Rat1 surface of Rai1 interaction (data not shown). Sequence alignment further revealed that the predicted nuclear localization signal of *S. pombe* Rat1 (TKKTK) (UniProt Consortium, 2012) is not conserved in *Tetrahymena* Xrn2. The lack of a nuclear localization signal could underlie the dependence of Xrn2 nuclear import on assembly with Twi12 RNP as TXT.

A major question is whether the Twi12-bound tRNA fragment can guide TXT to a target RNA substrate, as is the paradigm for Ago/Piwi RNPs. Twi12-bound sRNAs derive almost exclusively from a precise region of the sense strand of mature tRNAs that contains a bulky m^1A base modification (Figure 2C), which would disrupt the hydrogen-bonding surface of the seed sequence for target RNA recognition. If this base modification is sufficient to preclude sRNA pairing to any target RNA, sRNA binding by Twi12 may be required only to favor the Twi12 conformation that binds, stabilizes, imports to the nucleus, and catalytically activates Xrn2. Alternatively, in addition to those roles, Twi12 RNP could influence the affinity and/or specificity of cellular RNA selection as a substrate for Xrn2. Weak base-pairing of sRNA and target RNA could be optimal in order to balance target recruitment and its subsequent release to allow complete degradation.

In tRNA tertiary structure, the acceptor and T stems stack end on end to form a short duplex with the 3′ end of the tRNA as a single-stranded overhang, mimicking the features of a Dicer product. Notably, in *S. pombe dcr1Δ* cells, tRNA fragment representation in an Ago1-bound sRNA library is increased 5-fold, more so than rRNA (less than 2-fold) or mRNA (2-fold) (Halic and Moazed, 2010). This could be explained by tRNAs becoming the preferred substrate for Ago1 loading in the absence of Dicer products. Interestingly, deep sequencing reads matching tRNA fragments are found in most Ago/Piwi-bound sRNA libraries but are often filtered out before analysis. We suggest that there may be an evolutionarily broad Ago/Piwi-protein binding capacity for sRNAs derived from mature tRNAs. Beyond this potentially general Ago/Piwi loading with tRNA-derived sRNAs, it remains to be explored whether other Ago/Piwi proteins share the newly discovered Twi12 function of stimulating RNA processing in the nucleus.

EXPERIMENTAL PROCEDURES

Purifications

Affinity purifications from cell extract were performed largely as described (Couvillion and Collins, 2012). In brief, lysate was cleared at 16,000 × g for 15 min. Binding to rabbit IgG agarose (Sigma) or mouse anti-FLAG M2 resin (Sigma) was in 20 mM Tris-HCl (pH 7.5), 0.1 M NaCl, 10% glycerol, 0.2% Igepal, 0.1% Triton X-100, 1 mM $MgCl_2$, and protease inhibitors. Washes were in binding buffer with 0.1% Igepal, 0.1% Tween-20, and no Triton X-100. Complexes were eluted with TEV protease or 150 ng/μl triple FLAG peptide. So that Xrn2 depleted of Twi12 could be obtained, Xrn2-ZZ expression was induced by the addition of 250 μM $CuSO_4$ for the last 3 hr of culture growth. The proteasome inhibitor MG132 was added to cultures at a final concentration of 13 μM for the last 1 hr of culture growth, and 5 μM MG132 was added to cell lysate. For FLAG antibody depletion of IgG-purified samples, the TEV protease eluate was diluted 2-fold in binding buffer with 0.2 M NaCl and incubated with FLAG antibody resin for 30 min at room temperature. Bound complexes were eluted with triple FLAG peptide.

Activity Assays

For most exonuclease assays, complexes purified from *Tetrahymena* were incubated with ~1 μg *Tetrahymena* total low-molecular-weight RNA (Lee and Collins, 2006) in 10 mM Tris-HCl (pH 7.5), 50 mM KCl, and 1 mM $MgCl_2$ at 30°C for 60 min. For the assay in Figure 7E, complexes or proteins in limiting amounts were incubated with 25 ng each gel purified 5.8S rRNA and 5S rRNA in 20 mM Tris-HCl (pH 8.0), 100 mM NaCl, 5 mM $MgCl_2$, and 0.5 mM DTT at 30°C for 10 min. Time courses were also performed for verification of enzyme turnover (data not shown).

ACCESSION NUMBERS

GenBank accession numbers and *Tetrahymena* Genome Database annotations are as follows: *TWI12*, EF507507 and TTHERM_00653810; *XRN2*, XM_001011167.1 and TTHERM_00145270; and *TAN1*, XM_001014010.3 and TTHERM_00399370. The sRNA sequencing library is deposited in the Gene Expression Omnibus with the accession number GSE38507, as data set GSM943743.

SUPPLEMENTAL INFORMATION

Supplemental Information includes Supplemental Experimental Procedures and five figures and can be found with this article online at http://dx.doi.org/10.1016/j.molcel.2012.09.010.

ACKNOWLEDGMENTS

This work was supported by NIH grant GM54198 (K.C.) and a predoctoral fellowship from the Genentech Foundation (M.T.C.). We thank members of the Collins lab for helpful discussion and Emily Egan for critical reading of the manuscript.

Received: June 15, 2012
Revised: July 26, 2012
Accepted: September 7, 2012
Published online: October 18, 2012

REFERENCES

Andersen, K.L., and Collins, K. (2012). Several RNase T2 enzymes function in induced tRNA and rRNA turnover in the ciliate *Tetrahymena*. Mol. Biol. Cell *23*, 36–44.

Bayne, E.H., White, S.A., Kagansky, A., Bijos, D.A., Sanchez-Pulido, L., Hoe, K.L., Kim, D.U., Park, H.O., Ponting, C.P., Rappsilber, J., and Allshire, R.C. (2010). Stc1: a critical link between RNAi and chromatin modification required for heterochromatin integrity. Cell *140*, 666–677.

Brannan, K., Kim, H., Erickson, B., Glover-Cutter, K., Kim, S., Fong, N., Kiemele, L., Hansen, K., Davis, R., Lykke-Andersen, J., and Bentley, D.L. (2012). mRNA decapping factors and the exonuclease Xrn2 function in widespread premature termination of RNA polymerase II transcription. Mol. Cell *46*, 311–324.

Bühler, M., and Moazed, D. (2007). Transcription and RNAi in heterochromatic gene silencing. Nat. Struct. Mol. Biol. *14*, 1041–1048.

Burkhart, K.B., Guang, S., Buckley, B.A., Wong, L., Bochner, A.F., and Kennedy, S. (2011). A pre-mRNA-associating factor links endogenous siRNAs to chromatin regulation. PLoS Genet. *7*, e1002249.

Cernilogar, F.M., Onorati, M.C., Kothe, G.O., Burroughs, A.M., Parsi, K.M., Breiling, A., Lo Sardo, F., Saxena, A., Miyoshi, K., Siomi, H., et al. (2011). Chromatin-associated RNA interference components contribute to transcriptional regulation in *Drosophila*. Nature *480*, 391–395.

Chalker, D.L., and Yao, M.C. (2011). DNA elimination in ciliates: transposon domestication and genome surveillance. Annu. Rev. Genet. *45*, 227–246.

Chatterjee, S., and Grosshans, H. (2009). Active turnover modulates mature microRNA activity in *Caenorhabditis elegans*. Nature *461*, 546–549.

Couvillion, M.T., and Collins, K. (2012). Biochemical approaches including the design and use of strains expressing epitope-tagged proteins. Methods Cell Biol. *109*, 347–355.

Couvillion, M.T., Lee, S.R., Hogstad, B., Malone, C.D., Tonkin, L.A., Sachidanandam, R., Hannon, G.J., and Collins, K. (2009). Sequence, biogenesis, and function of diverse small RNA classes bound to the Piwi family proteins of *Tetrahymena thermophila*. Genes Dev. *23*, 2016–2032.

Couvillion, M.T., Sachidanandam, R., and Collins, K. (2010). A growth-essential *Tetrahymena* Piwi protein carries tRNA fragment cargo. Genes Dev. *24*, 2742–2747.

Davidson, L., Kerr, A., and West, S. (2012). Co-transcriptional degradation of aberrant pre-mRNA by Xrn2. EMBO J. *31*, 2566–2578.

Díaz, S., Amaro, F., Rico, D., Campos, V., Benítez, L., Martín-González, A., Hamilton, E.P., Orias, E., and Gutiérrez, J.C. (2007). *Tetrahymena* metallothioneins fall into two discrete subfamilies. PLoS ONE *2*, e291.

El Hage, A., Koper, M., Kufel, J., and Tollervey, D. (2008). Efficient termination of transcription by RNA polymerase I requires the 5′ exonuclease Rat1 in yeast. Genes Dev. *22*, 1069–1081.

Eulalio, A., Tritschler, F., and Izaurralde, E. (2009). The GW182 protein family in animal cells: new insights into domains required for miRNA-mediated gene silencing. RNA *15*, 1433–1442.

Geerlings, T.H., Vos, J.C., and Raué, H.A. (2000). The final step in the formation of 25S rRNA in Saccharomyces cerevisiae is performed by 5′−>3′ exonucleases. RNA *6*, 1698–1703.

Ghildiyal, M., and Zamore, P.D. (2009). Small silencing RNAs: an expanding universe. Nat. Rev. Genet. *10*, 94–108.

Gorovsky, M.A. (1973). Macro- and micronuclei of *Tetrahymena pyriformis*: a model system for studying the structure and function of eukaryotic nuclei. J. Protozool. *20*, 19–25.

Grewal, S.I. (2010). RNAi-dependent formation of heterochromatin and its diverse functions. Curr. Opin. Genet. Dev. *20*, 134–141.

Guang, S., Bochner, A.F., Burkhart, K.B., Burton, N., Pavelec, D.M., and Kennedy, S. (2010). Small regulatory RNAs inhibit RNA polymerase II during the elongation phase of transcription. Nature *465*, 1097–1101.

Gullerova, M., and Proudfoot, N.J. (2008). Cohesin complex promotes transcriptional termination between convergent genes in *S. pombe*. Cell *132*, 983–995.

Halic, M., and Moazed, D. (2010). Dicer-independent primal RNAs trigger RNAi and heterochromatin formation. Cell *140*, 504–516.

Haussecker, D., Huang, Y., Lau, A., Parameswaran, P., Fire, A.Z., and Kay, M.A. (2010). Human tRNA-derived small RNAs in the global regulation of RNA silencing. RNA *16*, 673–695.

Henry, Y., Wood, H., Morrissey, J.P., Petfalski, E., Kearsey, S., and Tollervey, D. (1994). The 5′ end of yeast 5.8S rRNA is generated by exonucleases from an upstream cleavage site. EMBO J. *13*, 2452–2463.

Ishizu, H., Nagao, A., and Siomi, H. (2011). Gatekeepers for Piwi-piRNA complexes to enter the nucleus. Curr. Opin. Genet. Dev. *21*, 484–490.

Jimeno-González, S., Haaning, L.L., Malagon, F., and Jensen, T.H. (2010). The yeast 5′-3′ exonuclease Rat1p functions during transcription elongation by RNA polymerase II. Mol. Cell *37*, 580–587.

Jinek, M., Coyle, S.M., and Doudna, J.A. (2011). Coupled 5′ nucleotide recognition and processivity in Xrn1-mediated mRNA decay. Mol. Cell *41*, 600–608.

Juliano, C., Wang, J., and Lin, H. (2011). Uniting germline and stem cells: the function of Piwi proteins and the piRNA pathway in diverse organisms. Annu. Rev. Genet. *45*, 447–469.

Kaneko, S., Rozenblatt-Rosen, O., Meyerson, M., and Manley, J.L. (2007). The multifunctional protein p54nrb/PSF recruits the exonuclease XRN2 to facilitate pre-mRNA 3′ processing and transcription termination. Genes Dev. *21*, 1779–1789.

Kawaoka, S., Izumi, N., Katsuma, S., and Tomari, Y. (2011). 3′ end formation of PIWI-interacting RNAs in vitro. Mol. Cell *43*, 1015–1022.

Kawauchi, J., Mischo, H., Braglia, P., Rondon, A., and Proudfoot, N.J. (2008). Budding yeast RNA polymerases I and II employ parallel mechanisms of transcriptional termination. Genes Dev. *22*, 1082–1092.

Kim, M., Krogan, N.J., Vasiljeva, L., Rando, O.J., Nedea, E., Greenblatt, J.F., and Buratowski, S. (2004). The yeast Rat1 exonuclease promotes transcription termination by RNA polymerase II. Nature *432*, 517–522.

Kwak, P.B., and Tomari, Y. (2012). The N domain of Argonaute drives duplex unwinding during RISC assembly. Nat. Struct. Mol. Biol. *19*, 145–151.

Lee, S.R., and Collins, K. (2006). Two classes of endogenous small RNAs in *Tetrahymena thermophila*. Genes Dev. *20*, 28–33.

Liang, X.H., and Crooke, S.T. (2011). Depletion of key protein components of the RISC pathway impairs pre-ribosomal RNA processing. Nucleic Acids Res. *39*, 4875–4889.

Luo, W., Johnson, A.W., and Bentley, D.L. (2006). The role of Rat1 in coupling mRNA 3′-end processing to transcription termination: implications for a unified allosteric-torpedo model. Genes Dev. *20*, 954–965.

Ma, J.B., Yuan, Y.R., Meister, G., Pei, Y., Tuschl, T., and Patel, D.J. (2005). Structural basis for 5′-end-specific recognition of guide RNA by the *A. fulgidus* Piwi protein. Nature *434*, 666–670.

Miao, W., Xiong, J., Bowen, J., Wang, W., Liu, Y., Braguinets, O., Grigull, J., Pearlman, R.E., Orias, E., and Gorovsky, M.A. (2009). Microarray analyses of gene expression during the *Tetrahymena thermophila* life cycle. PLoS ONE *4*, e4429.

Moshkovich, N., Nisha, P., Boyle, P.J., Thompson, B.A., Dale, R.K., and Lei, E.P. (2011). RNAi-independent role for Argonaute2 in CTCF/CP190 chromatin insulator function. Genes Dev. *25*, 1686–1701.

Noto, T., Kurth, H.M., Kataoka, K., Aronica, L., DeSouza, L.V., Siu, K.W., Pearlman, R.E., Gorovsky, M.A., and Mochizuki, K. (2010). The *Tetrahymena* argonaute-binding protein Giw1p directs a mature argonaute-siRNA complex to the nucleus. Cell *140*, 692–703.

Olivieri, D., Sykora, M.M., Sachidanandam, R., Mechtler, K., and Brennecke, J. (2010). An in vivo RNAi assay identifies major genetic and cellular requirements for primary piRNA biogenesis in *Drosophila*. EMBO J. *29*, 3301–3317.

Orban, T.I., and Izaurralde, E. (2005). Decay of mRNAs targeted by RISC requires XRN1, the Ski complex, and the exosome. RNA *11*, 459–469.

Phizicky, E.M., and Alfonzo, J.D. (2010). Do all modifications benefit all tRNAs? FEBS Lett. *584*, 265–271.

Ramachandran, V., and Chen, X. (2008). Degradation of microRNAs by a family of exoribonucleases in *Arabidopsis*. Science *321*, 1490–1492.

Rehwinkel, J., Behm-Ansmant, I., Gatfield, D., and Izaurralde, E. (2005). A crucial role for GW182 and the DCP1:DCP2 decapping complex in miRNA-mediated gene silencing. RNA *11*, 1640–1647.

Rüdel, S., Wang, Y., Lenobel, R., Körner, R., Hsiao, H.H., Urlaub, H., Patel, D., and Meister, G. (2011). Phosphorylation of human Argonaute proteins affects small RNA binding. Nucleic Acids Res. *39*, 2330–2343.

Seto, A.G., Kingston, R.E., and Lau, N.C. (2007). The coming of age for Piwi proteins. Mol. Cell *26*, 603–609.

Souret, F.F., Kastenmayer, J.P., and Green, P.J. (2004). AtXRN4 degrades mRNA in *Arabidopsis* and its substrates include selected miRNA targets. Mol. Cell *15*, 173–183.

Thompson, D.M., and Parker, R. (2009). Stressing out over tRNA cleavage. Cell *138*, 215–219.

Tolia, N.H., and Joshua-Tor, L. (2007). Slicer and the argonautes. Nat. Chem. Biol. *3*, 36–43.

UniProt Consortium. (2012). Reorganizing the protein space at the Universal Protein Resource (UniProt). Nucleic Acids Res. *40* (Database issue), D71–D75.

Wang, M., and Pestov, D.G. (2011). 5′-end surveillance by Xrn2 acts as a shared mechanism for mammalian pre-rRNA maturation and decay. Nucleic Acids Res. *39*, 1811–1822.

West, S., Gromak, N., and Proudfoot, N.J. (2004). Human 5′ —> 3′ exonuclease Xrn2 promotes transcription termination at co-transcriptional cleavage sites. Nature *432*, 522–525.

Woolcock, K.J., Stunnenberg, R., Gaidatzis, D., Hotz, H.R., Emmerth, S., Barraud, P., and Bühler, M. (2012). RNAi keeps Atf1-bound stress response genes in check at nuclear pores. Genes Dev. *26*, 683–692.

Xiang, S., Cooper-Morgan, A., Jiao, X., Kiledjian, M., Manley, J.L., and Tong, L. (2009). Structure and function of the 5′—>3′ exoribonuclease Rat1 and its activating partner Rai1. Nature *458*, 784–788.

Xue, Y., Bai, X., Lee, I., Kallstrom, G., Ho, J., Brown, J., Stevens, A., and Johnson, A.W. (2000). *Saccharomyces cerevisiae* RAI1 (YGL246c) is homologous to human DOM3Z and encodes a protein that binds the nuclear exoribonuclease Rat1p. Mol. Cell. Biol. *20*, 4006–4015.

Ye, R., Wang, W., Iki, T., Liu, C., Wu, Y., Ishikawa, M., Zhou, X., and Qi, Y. (2012). Cytoplasmic assembly and selective nuclear import of *Arabidopsis* Argonaute4/siRNA complexes. Mol. Cell *46*, 859–870.

Zaratiegui, M., Castel, S.E., Irvine, D.V., Kloc, A., Ren, J., Li, F., de Castro, E., Marín, L., Chang, A.Y., Goto, D., et al. (2011). RNAi promotes heterochromatic silencing through replication-coupled release of RNA Pol II. Nature *479*, 135–138.

Molecular Cell, Volume *48*

Supplemental Information

A *Tetrahymena* Piwi Bound to Mature tRNA 3′ Fragments Activates the Exonuclease Xrn2 for RNA Processing in the Nucleus

Mary T. Couvillion, Gergana Bounova, Elizabeth Purdom, Terence P. Speed, and Kathleen Collins

SUPPLEMENTAL EXPERIMENTAL PROCEDURES

Cell lines

Cell lines overexpressing tagged Twi12 or Twi12 variants were made using integration cassettes targeted to the *BTU1* locus in strain CU522. The endogenous open reading frame (ORF), or ORF modified by DpnI-mediated site-directed mutagenesis, was fused to an N-terminal ZZ-TEV-3×FLAG (ZZF) tag as described in the text. The tag was preceded by an ~1 kbp promoter region from *MTT1* (Shang et al., 2002), and the ORF was followed by the polyadenylation signal of *BTU1*. Cells were selected using paclitaxel (Witkin and Collins, 2004). Following paclitaxel selection, the endogenous *TWI12* locus was targeted for replacement with the *neo2* cassette and cells were selected for maximal assortment using paromomycin (Witkin et al., 2007).

Cell lines expressing endogenously tagged Twi12 or Twi12 variants were made using integration cassettes targeted to the *TWI12* locus in strain CU522. The endogenous or mutated ORF and ~150 bp following the stop codon (including the endogenous 3' UTR and polyadenylation signal) were fused to an N-terminal tag as described. The *neo2* cassette was integrated after the ORF and downstream region and cells were selected for maximal assortment using paromomycin (Witkin et al., 2007).

Cell lines expressing endogenously tagged Tan1 and Xrn2 were made using integration cassettes targeted to the respective locus in strain CU522 as for Twi12. For C-terminal tagging, 3×FLAG-TEV-ZZ (FZZ) was integrated just before the stop codon, followed by ~300 bp of endogenous downstream region (including the endogenous 3' UTR and polyadenylation signal) then the *neo2* cassette. For N-terminal tags, ZZF was preceded by ~500 bp of the region just upstream of the start codon (including the endogenous 5' UTR and the endogenous promoter sequence); *neo2* was integrated just upstream of this. Cells were selected for maximal assortment using paromomycin, and assortment was monitored by PCR using primers across the tag. C-terminally tagged Tan1 was purified with marginally more recovery from cell extracts than N-terminally tagged Tan1. Tan1 knockout and Xrn2 knockdown lines were made in CU522 background as described for *TWI12* locus replacement above.

Cell lines in which expression of Twi12 or Xrn2 can be inducibly depleted were made in *TWI12:neo2* or *XRN2:neo2* backgrounds, respectively, in strain CU522. Integration cassettes were targeted to the *MTT3* locus, so that the transgene would be under the control of the cadmium-inducible *MTT3* promoter (Diaz et al., 2007). For Twi12 iKD, the endogenous Twi12 ORF was fused to an N-terminal 3×FLAG tag (F), and the ORF was followed by the polyadenylation signal of *BTU1* then the *bsr2* cassette (Couvillion and Collins, 2012). For Xrn2 iKD, the strategy was the same except the tag was C-terminal, and the integrated *XRN2* gene

contained introns. Cells were selected initially in the presence of cadmium using blasticidin, and cadmium was subsequently diluted by daily passaging. After 5 to 6 days of passaging in maximum tolerated blasticidin concentration, cells were passaged out of drug for one day, then selected for maximal assortment of *TWI12:neo2* or *XRN2:neo2* using paromomycin in the presence of cadmium to support expression of the transgene. Twi12 iKD was maintained in 0.7 μg/mL $CdCl_2$, and Xrn2 iKD was maintained in 0.1 μg/mL $CdCl_2$. For inducible knockdown, cells were washed out of cadmium-containing media, inoculated at 2 - 4 × 10^3 cells/mL and allowed to double 5 to 7 times before collecting.

The cell line expressing tagged Xrn2 in the Twi12 iKD background was made using an integration cassette targeted to the *BTU1* locus. The *XRN2* gene, containing introns, was fused to a C-terminal *ZZ* tag, followed by the polyadenylation signal of *BTU1*. The start codon of the *XRN2* gene was preceded by an ~1 kbp promoter region from the copper-inducible *MTT2* gene (Boldrin et al., 2008). Cells were selected using paclitaxel (Witkin and Collins, 2004). Transgene expression was induced overnight using a $CuSO_4$ concentration of 50 - 500 μM, unless otherwise noted.

DNA, RNA, and protein assays

Southern blots and mRNA Northern blots were hybridized with hexamer-primed probes. Northern blots for pre-rRNA, rRNA, and tRNA used 5'-end radiolabeled oligonucleotide probes. Probe sequences for rRNA detection are as follows (from left to right in the schematic of Figure 6B): 5'-CCATTCGCAGTTTCGCTGTTCAATACTGAACTGGCACATG -3', 5'-CGTTTTGGATGTTATCCAGATCTTAGAC -3', 5'- TTCCACACTGAAACAAACATGA -3'. The probe sequence for tRNA detection are: $tRNA^{Ala}$ 5'- TGGAGAACCTGGGCATTGAT -3', $tRNA^{Gly}$ 5'- TGCACCGACCGGGAATCGAAG -3'.

Western blots were performed as described (Couvillion and Collins, 2012). For mass spectrometry, complexes were eluted in 8 M urea after the second affinity purification and processed as described previously (Fu and Collins, 2007). For pyrophosphohydrolase assays, complexes or proteins were incubated with 50 ng gel-purified 70 nt 5' triphosphorylated RNA from in vitro transcription. Reaction buffer was 10 mM Tris-HCl, pH 7.5, 100 mM potassium acetate, 2 mM magnesium acetate, 0.5 mM $MnCl_2$, 2 mM DTT. Reactions proceeded at 37°C for 30 min. Products were resolved by 9% 9:1 acrylamide:bis-acrylamide urea PAGE to separate RNAs with different numbers of 5' phosphates (Pak and Fire, 2007).

Small RNA library preparation, sequencing, and analysis

Twi12-associated RNA in the size ranges of ~10-12 nt, ~18-22 nt, and ~23-25 nt were gel-purified and prepared separately for Illumina deep sequencing as described (Couvillion et al., 2009), then mixed for sequencing in one lane of a Genome Analyzer IIx. Filtered reads 16-22 nt in length were used for mapping.

The sRNA library consisting of 17,756,697 36-nt reads was trimmed of 3' adaptor by searching between positions 9 and 29 and constraining sRNA length to be between 8 and 28 nt long. The adaptor was found with 0 mismatches in 68% of sequences, and with up to 2 mismatches in 98.5% of sequences. In the remaining set of reads, the search was relaxed by requiring only the first six nucleotides of the adaptor to be an exact match, resulting in 99.1% of usable reads. For the set of invalid reads (0.89%), the adaptor was either found too early (small RNA <8 nt) or with too many mismatches, due to lower read quality. Cloned RNA lengths of 16-22 nt constituted 77% of the trimmed reads.

Because of the short length of reads in this dataset and the extensive similarity within and between tRNA isoacceptor genes to which a majority of reads mapped, it would be ideal to allow for zero mismatches. This is not practical however due to the existence of tRNA base modifications. In this data, modifications were manifested as a high frequency of mismatch at the modification site. Since tRNA base modification sites are not experimentally confirmed for *Tetrahymena*, mismatch frequency was used to detect potential sites of modification based on the assumption that the base swap frequencies at any given nucleotide position are different from those at a modification site. First, for every base position in every tRNA gene, we calculated the number of perfect matches (e.g. A to A) and the number of mismatches and frequency of each base swap (e.g. A to T, A to C, and A to G) if there were mismatches. A binomial test with expected fraction of correct swap of 0.99 was performed for all positions and then the p-values were corrected using a false discovery rate method. A cutoff p-value of 10^{-15} was selected so that the average number of proposed modifications per gene is 3.5, based on the median value of 8 modifications per tRNA across all characterized tRNA species (Phizicky and Alfonzo, 2010), and an estimate that less than half of those will cause reverse transcriptase to incorporate the wrong nucleotide rather than stop or make no error. Note that the reads in the data are highly biased towards the tRNA 3' and 5' ends, so they do not cover the genes uniformly and thus will not be useful for detection of all possible modifications. The modifications determined based on the binomial test became pre-defined modification positions. We then defined an *allowable mismatch* alignment to be an alignment with a mismatch only at a pre-defined modification position.

For the mapping and annotation presented in Figures 1C and 2A, we first divided reads into two bins: those that end in C, CC, or CCA, and those that do not. For each bin the following procedure was used. First steps 1-6 listed below were performed requiring a perfect match, then repeated allowing for one mismatch. Reads mapping to tRNAs with one mismatch were annotated as tRNA only if the position was a site of modification, and for all other categories a mismatch was allowed at any position.

1) Map reads to **tRNA genes**. Use unmapped reads in the next step.
2) Map reads to **mRNA genes** (annotated genes in the genome). Split the aligned reads into exon or intron mappers and intergenic mappers.
3) Map intergenic mappers from above to other **non-coding RNA** (snRNA, snoRNA, 5S rRNA, telomerase). Use unmapped reads in the next step.
4) Map reads to **tRNA introns** (11 genes out of 129 have introns). The unmapped reads from this step are reads that map purely to intergenic regions.
5) Map the unmapped reads from step 2 to the **ribosomal DNA**. Use the unmapped reads for the next step.
6) Map reads to the **mitochondial DNA**. Use the unmapped reads to repeat step 1-6 once allowing for one mismatch, then move on to step 7.
7) Strip remaining unmapped reads ending in C, CC, or CCA of those nucleotides and repeat steps 1-6.

Two-dimensional thin layer chromatography

The 23-24 nt sRNA and full-length tRNA were gel purified from *Tetrahymena* cellular RNA. Twi12-bound RNA was obtained from a one-step IgG IP of ZZF-Twi12 overexpressed from the uninduced *MTT1* promoter. Purified RNA samples were processed as described previously (Grosjean et al., 2007). After complete digestion with RNase T2, the 3' mononucleosides were ^{32}P-labeled to create 3',5' -diphosphate nucleosides. The 3' phosphate was removed by treatment

with nuclease P1. The labeled 5'-monophosphate nucleosides were spotted onto cellulose plates. The solvent for the first dimension, run overnight, was 66:1:3 (v:v:v) isobutyric acid: 25% ammonia (NH_4OH): water, with 1 mM EDTA, pH 8.0. The solvent for the second dimension, run overnight, was 100:60:2 (v:w:v) 0.1 M sodium phosphate, pH 6.8: ammonium phosphate (NH_4SO_4): 1-propanol.

Fluorescence microscopy

Cells were washed in 10 mM Tris-HCl, pH 7.5, fixed in 2% paraformaldehyde in PHEM buffer (Schliwa and van Blerkom, 1981), and permeabilized in 0.2% Triton X-100 in PHEM buffer. For immunofluorescence, cells were incubated with primary antibody and 0.1% BSA, 3% normal goat serum, and 0.1% Tween-20 in modified PBS (8 mM Na_2HPO_4, 2 mM KH_2PO_4, 130 mM NaCl, 2 mM KCl, 10 mM EGTA, 2 mM $MgCl_2$), pH 7.2 overnight at 4°C, and with secondary antibody for 1 h at room temperature. For direct nucleic acid staining, fixed and permeabilized cells were incubated with 500 nM SYTO RNASelect (Invitrogen) in modified PBS for 30 minutes at room temperature. Cells were stained with 10 ng/mL DAPI for 5 minutes at room temperature. Fluorescence was visualized using the 40× objective of an Olympus model BX61 microscope equipped with a Hamamatsu Digital camera. Images were captured using Metamorph software.

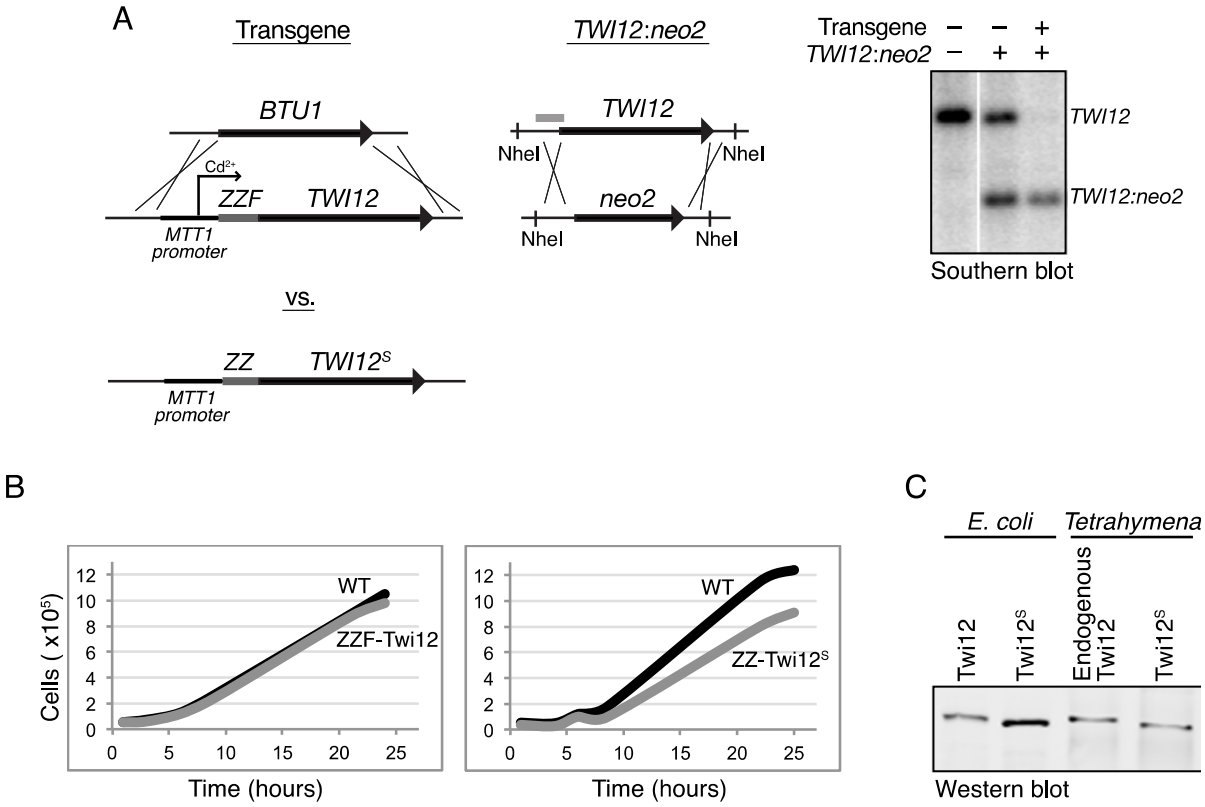

Figure S1. Tagged full-length Twi12 is functional and supports wild-type growth, Related to Figure 1

(A) Schematic showing ZZF-Twi12 transgene integration and endogenous *TWI12* locus knockout. The latter is evidenced by Southern blotting at right using NheI-digested genomic DNA. The position of the Southern blot probe is indicated in the *TWI12* locus schematic with a gray line. *TWI12* knockout was confirmed by reverse transcription and PCR (RT-PCR).

(B) Growth curves comparing wild type cell cultures to those expressing ZZF-Twi12 or ZZ-Twi12^S from the undinduced *MTT1* promoter and without endogenous Twi12. Timepoints were taken at 1, 3, 6, 9, 21, 24 hours and 1, 4, 6, 9, 22, 25 hours, respectively.

(C) Western blot probed with anti-Twi12 antibody comparing migration of Twi12 and Twi12^S. Untagged Twi12 and Twi12^S were expressed in *E. coli* and total protein was subjected to SDS-PAGE, or Tan1-FZZ and ZZ-Twi12^S were purified from *Tetrahymena* by one-step IgG IP and the TEV protease elution was subjected to SDS-PAGE. The migration of endogenous Twi12 coimmunoprecipitated with Tan1-FZZ matches the migration of the longer Twi12 version.

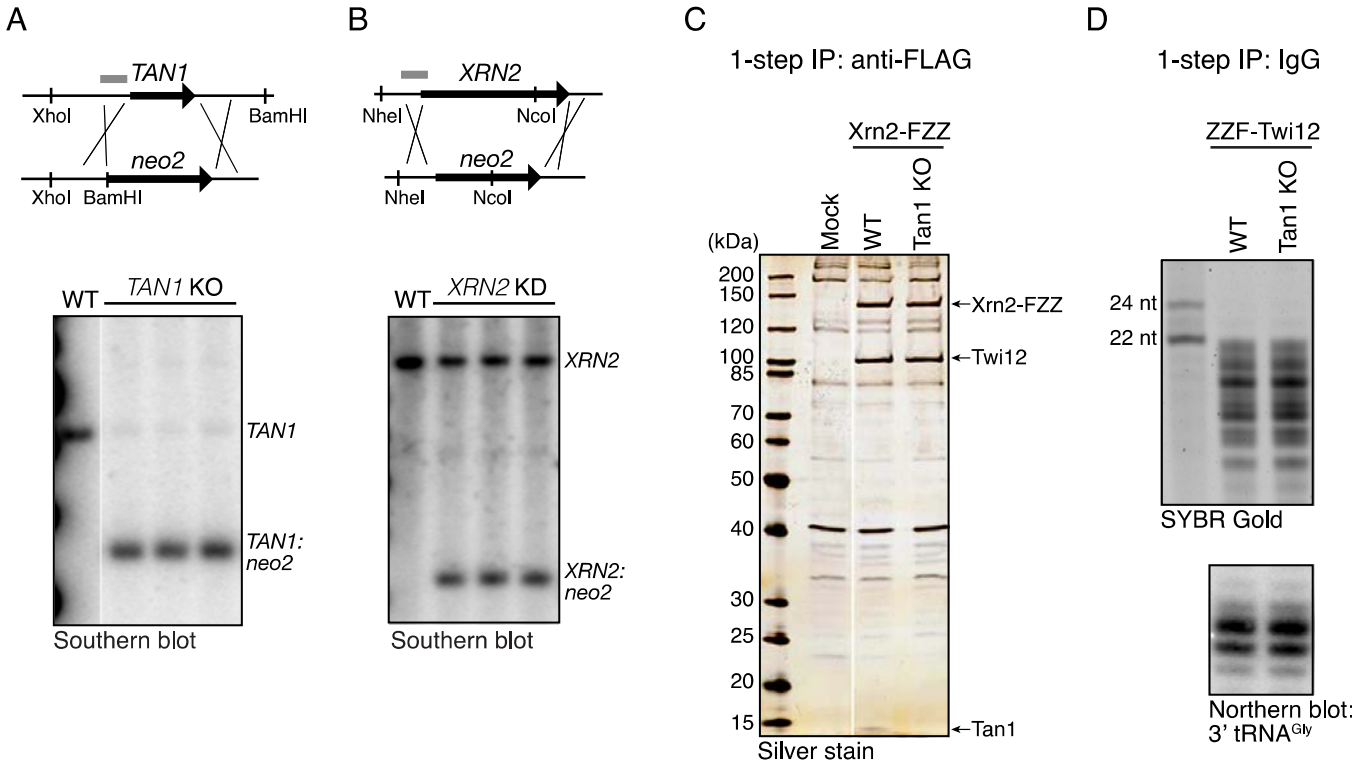

Figure S2. Tan1 is not essential, unlike Twi12 and Xrn2, and is not required for Twi12 association with Xrn2 or sRNA, Related to Figure 3

(A) Schematic showing endogenous *TAN1* locus targeting with a drug resistance cassette and Southern blotting using XhoI- and BamHI-digested genomic DNA. The position of the Southern blot probe is indicated by a gray line in the schematic. *TAN1* knockout was confirmed by RT-PCR.

(B) Schematic showing endogenous *XRN2* locus targeting with a drug resistance cassette and Southern blotting using NheI- and NcoI-digested genomic DNA. The position of the Southern blot probe is indicated by a gray line in the schematic.

(C) SDS-PAGE and silver staining after one-step IP of Xrn2-FZZ in cell lines with and without Tan1.

(D) RNA coimmunoprecipitated with ZZF-Twi12, in cell lines with and without Tan1, resolved by urea-PAGE and stained by SYBR Gold (top), and then probed to detect the 3' end of $tRNA^{Gly}$ (bottom).

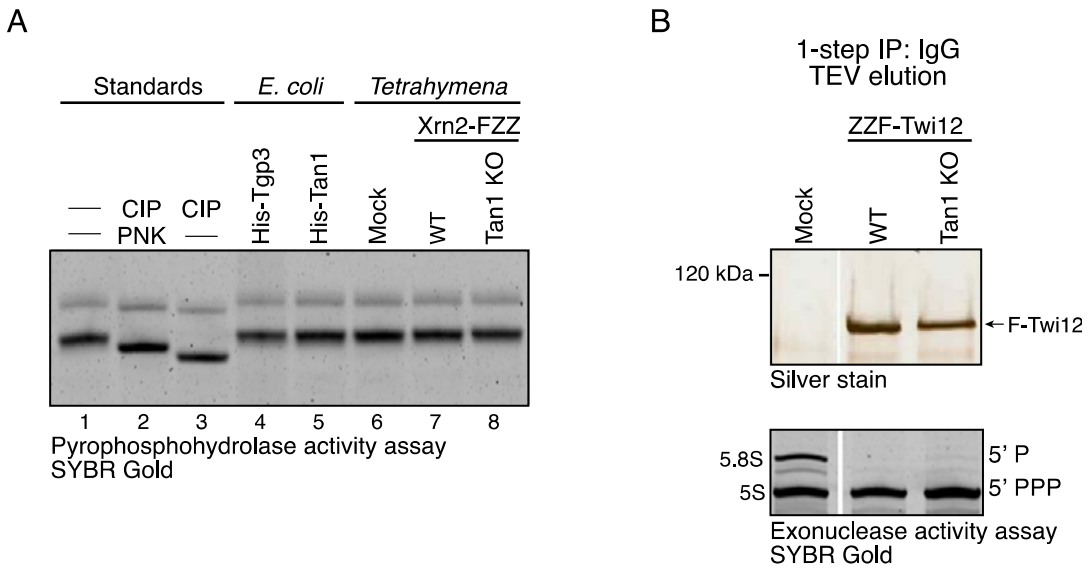

Figure S3. Tan1 does not have pyrophosphohydrolase activity nor does it affect Xrn2 activity in vitro, Related to Figure 4

(A) In vitro pyrophosphohydrolase activity assay on recombinant N-terminally 6×His-tagged Tan1 purified from *E. coli* (lane 5) with similarly tagged and purified recombinant *Tetrahymena* DNA binding protein Tgp3 as a negative control (lane 4), and on Tan1 purified from *Tetrahymena* in the context of TXT (via Xrn2-FZZ expressed from the endogenous *XRN2* promoter, lane 7) with IPs from cells lacking tagged protein (Mock, lane 6) or Tan1 KO cells (lane 8) as negative controls. The substrate is a 70 nt 5' triphosphorylated RNA, obtained by in vitro transcription with T7 RNA polymerase. For standards, the same RNA was left untreated (5' PPP, lane 1), treated with calf intestinal phosphatase (CIP, New England Biolabs) followed by polynucleotide kinase (PNK, New England Biolabs) (5' P, lane 2), or treated with CIP alone (5' OH, lane 3).

(B) Activity assay on TXT purified by ZZF-Twi12, in cell lines with and without Tan1. Top panel: silver stained F-Twi12 after one-step IP. Twi12 was overexpressed and purified in excess of Xrn2; the silver stain was not developed long enough to detect Xrn2. Bottom panel: RNA after in vitro incubation with each TEV protease elution as in Figure 4B.

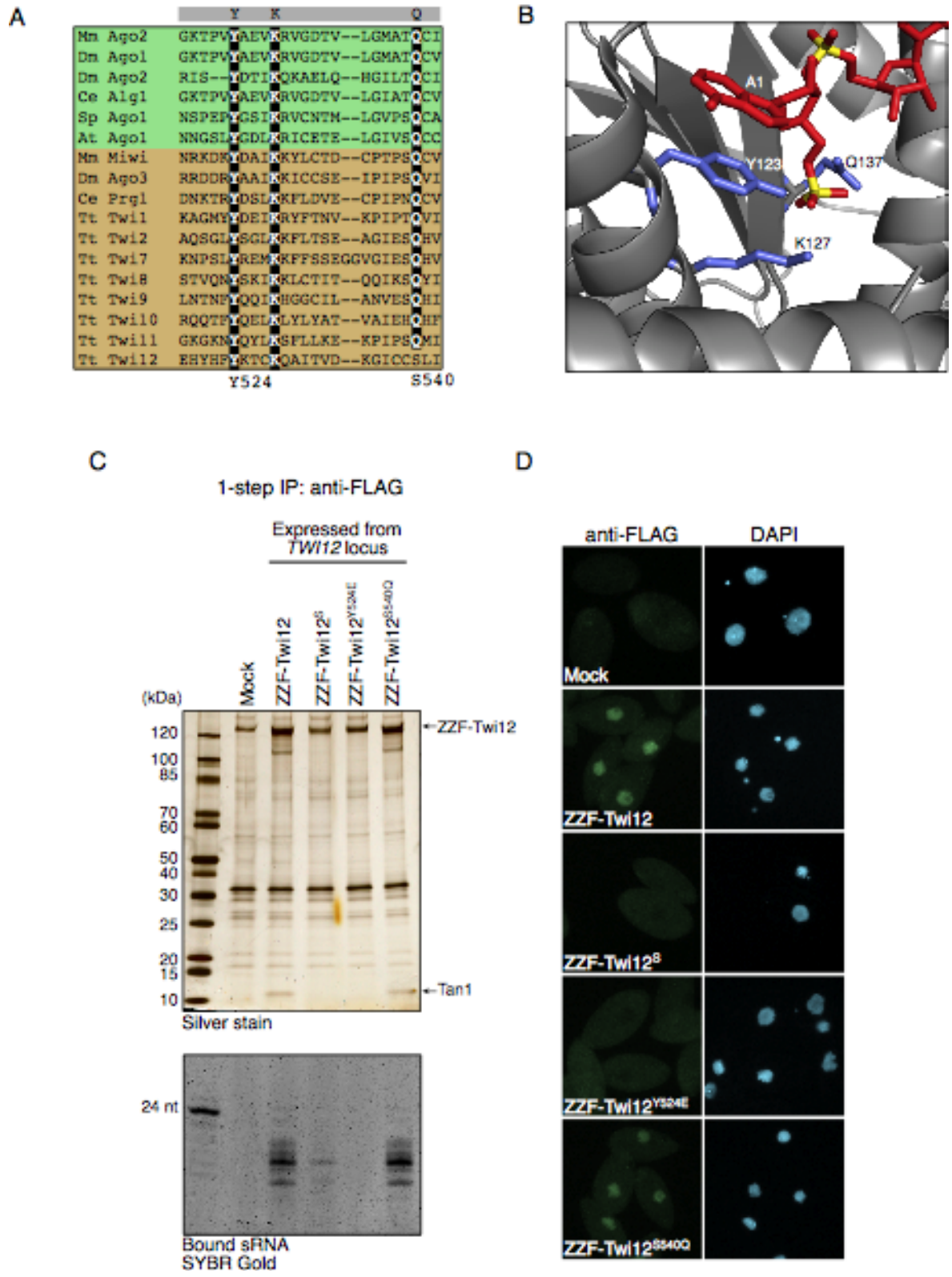

Figure S4. Twi12 nuclear localization is dependent on sRNA binding, Related to Figure 5
(A) Alignment of a region of Ago/Piwi MID domains containing conserved residues (highlighted) involved in anchoring the sRNA 5' phosphate (Ma et al., 2005). Argonaute proteins are shaded in

green and Piwi proteins are shaded in orange. Positions of the residues mutated in Twi12 are noted at the bottom. Mm, *Mus musculus*; Dm, *Drosophila melanogaster*; Ce, *Caenorhabditis elegans*; Sp, *Schizosaccharomyces pombe*; At, *Arabidopsis thaliana*; Tt, *Tetrahymena thermophila*. Modified from Bouhouche et al., 2011.
(B) Crystal structure of the *Archaeoglobus fulgidas* Piwi 5'-phosphate-binding pocket (Ma et al., 2005). Residues highlighted in (A) are marked. A1 is the base of 5' nucleotide of the bound RNA.
(C) SDS-PAGE and silver staining after one-step IP of ZZF-Twi12 wild-type and variants expressed from the *TWI12* promoter (top), and SYBR Gold-stained associated sRNA (bottom). Note the prominent background band comigrating with ZZF-Twi12 in the mock purification, which leads to visual overestimation of the amounts of ZZF-Twi12^{S} and ZZF-Twi12^{Y524E} that was purified. These two variants did purify, however, as evidenced by RNA co-purifying with ZZF-Twi12^{S}.
(D) Indirect IF for ZZF-Twi12 wild-type and variants expressed from the *TWI12* promoter.

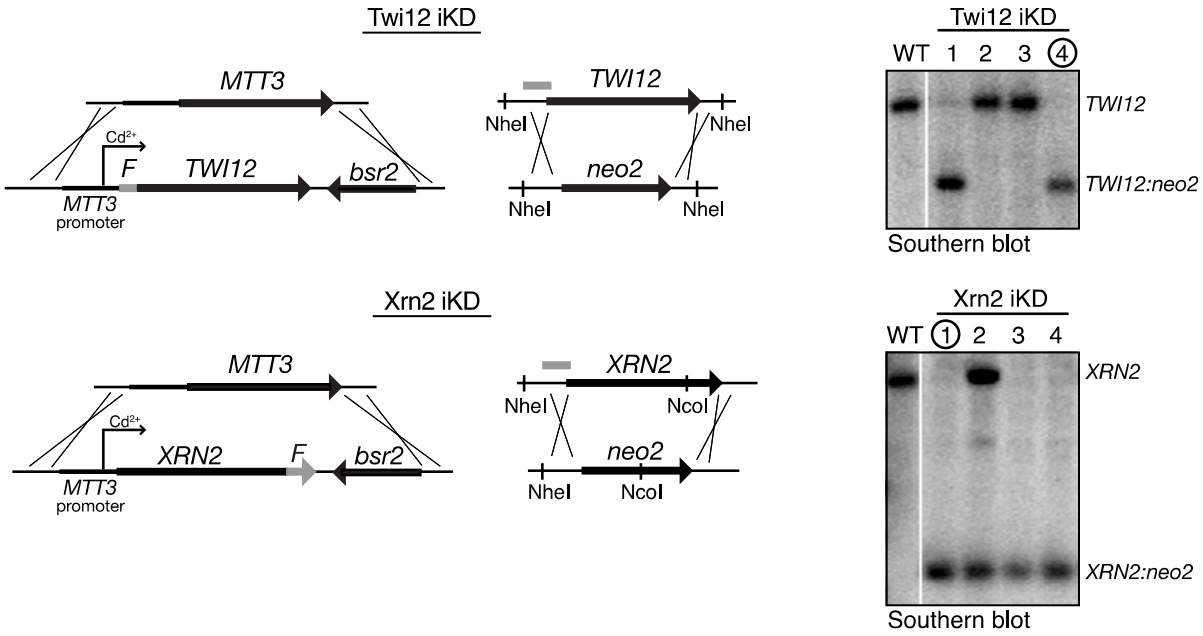

Figure S5. Strain construction for Twi12 or Xrn2 regulated depletion, Related to Figure 6
Schematic showing full targeting strategy for generating Twi12 iKD and Xrn2 iKD cell lines. The Southern blots at right show the extent of endogenous locus replacement with a drug resistance cassette in four independently selected populations for each line. The positions of the Southern blot probes are indicated in the locus schematics with a gray line. Circles indicate the populations used for experiments. *TWI12* and *XRN2* locus knockouts in these populations were confirmed by RT-PCR.

SUPPLEMENTAL REFERENCES

Boldrin, F., Santovito, G., Formigari, A., Bisharyan, Y., Cassidy-Hanley, D., Clark, T.G., and Piccinni, E. (2008). *MTT2*, a copper-inducible metallothionein gene from *Tetrahymena thermophila*. Comp Biochem Physiol C Toxicol Pharmacol *147*, 232-240.

Bouhouche, K., Gout, J.F., Kapusta, A., Betermier, M., and Meyer, E. (2011). Functional specialization of Piwi proteins in *Paramecium tetraurelia* from post-transcriptional gene silencing to genome remodelling. Nucleic Acids Res *39*, 4249-4264.

Fu, D., and Collins, K. (2007). Purification of human telomerase complexes identifies factors involved in telomerase biogenesis and telomere length regulation. Mol Cell *28*, 773-785.

Grosjean, H., Droogmans, L., Roovers, M., and Keith, G. (2007). Detection of enzymatic activity of transfer RNA modification enzymes using radiolabeled tRNA substrates. Methods Enzymol *425*, 55-101.

Pak, J., and Fire, A. (2007). Distinct populations of primary and secondary effectors during RNAi in *C. elegans*. Science *315*, 241-244.

Schliwa, M., and van Blerkom, J. (1981). Structural interaction of cytoskeletal components. J Cell Biol *90*, 222-235.

Shang, Y., Song, X., Bowen, J., Corstanje, R., Gao, Y., Gaertig, J., and Gorovsky, M.A. (2002). A robust inducible-repressible promoter greatly facilitates gene knockouts, conditional expression, and overexpression of homologous and heterologous genes in *Tetrahymena thermophila*. Proc Natl Acad Sci USA *99*, 3734-3739.

Witkin, K.L., and Collins, K. (2004). Holoenzyme proteins required for the physiological assembly and activity of telomerase. Genes Dev *18*, 1107-1118.

Witkin, K.L., Prathapam, R., and Collins, K. (2007). Positive and negative regulation of *Tetrahymena* telomerase holoenzyme. Mol Cell Biol *27*, 2074-2083.